https://doi.org/10.5194/mr-2021-58
Preprint. Discussion started: 20 July 2021

Open Access MAGNETIC RESONANCE Discussions

Rapid measurement of Watson-Crick to Hoogsteen exchange in unlabeled DNA duplexes using high-power SELOPE imino ^{1}H CEST

Bei Liu[1], Atul Rangadurai[1], Honglue Shi[2], and Hashim M. Al-Hashimi*[1,2]

1. Department of Biochemistry, Duke University School of Medicine, Durham, NC, USA

2. Department of Chemistry, Duke University, Durham, NC, USA

**Correspondence to: hashim.al.hashimi@duke.edu*

https://doi.org/10.5194/mr-2021-58
Preprint. Discussion started: 20 July 2021

Open Access MAGNETIC RESONANCE Discussions

Abstract. In duplex DNA, Watson-Crick A-T and G-C base pairs (bps) exist in dynamic equilibrium with an alternative Hoogsteen conformation, which is low in abundance and short-lived. Measuring how the Hoogsteen dynamics varies across different DNA sequences, structural contexts and physiological conditions is key for understanding the role of these non-canonical bps in DNA recognition and repair. However, such studies are hampered by the need to prepare ^{13}C or ^{15}N isotopically enriched DNA samples for NMR relaxation dispersion (RD) experiments. Here, using SELective Optimized Proton Experiments (SELOPE) ^{1}H CEST experiments employing high-power radiofrequency fields (B_1 > 250 Hz) targeting imino protons, we demonstrate accurate and robust characterization of Waston-Crick to Hoogsteen exchange, without the need for isotopic enrichment of the DNA. For 13 residues in three DNA duplexes under different temperature and pH conditions, the exchange parameters deduced from high-power imino ^{1}H CEST were in very good agreement with counterparts measured using off-resonance $^{13}C/^{15}N$ spin relaxation in the rotating frame ($R_{1\rho}$). It is shown that ^{1}H-^{1}H NOE effects which typically introduce artifacts in ^{1}H based measurements of chemical exchange can be effectively suppressed by selective excitation, provided that the relaxation delay is short (≤100 ms). The ^{1}H CEST experiment can be performed with ~10X higher throughput and ~100X lower cost relative to $^{13}C/^{15}N$ $R_{1\rho}$, and enabled Hoogsteen chemical exchange measurements undetectable by $R_{1\rho}$. The

https://doi.org/10.5194/mr-2021-58
Preprint. Discussion started: 20 July 2021

Open Access MAGNETIC RESONANCE Discussions

results reveal an increased propensity to form Hoogsteen bps near terminal ends and a diminished propensity within A-tract motifs. The ^{1}H CEST experiment opens the door to more comprehensively characterizing Hoogsteen breathing in duplex DNA.

https://doi.org/10.5194/mr-2021-58
Preprint. Discussion started: 20 July 2021


Open Access MAGNETIC RESONANCE Discussions

1 Introduction

Soon after the discovery of the DNA double helix, it was shown that A-T and G-C could also pair in an alternative conformation known as the “Hoogsteen” base pair (bp) (Felsenfeld et al., 1957; Hoogsteen, 1959) (Fig. 1a). Starting from a canonical Watson-Crick G-C or A-T bp, the corresponding Hoogsteen bp can be obtained by flipping the purine base 180º and bringing the two bases into proximity to create a new set of hydrogen-bonds, which in the case of G-C bps require protonation of cytosine-N3 (Fig. 1a).

https://doi.org/10.5194/mr-2021-58
Preprint. Discussion started: 20 July 2021

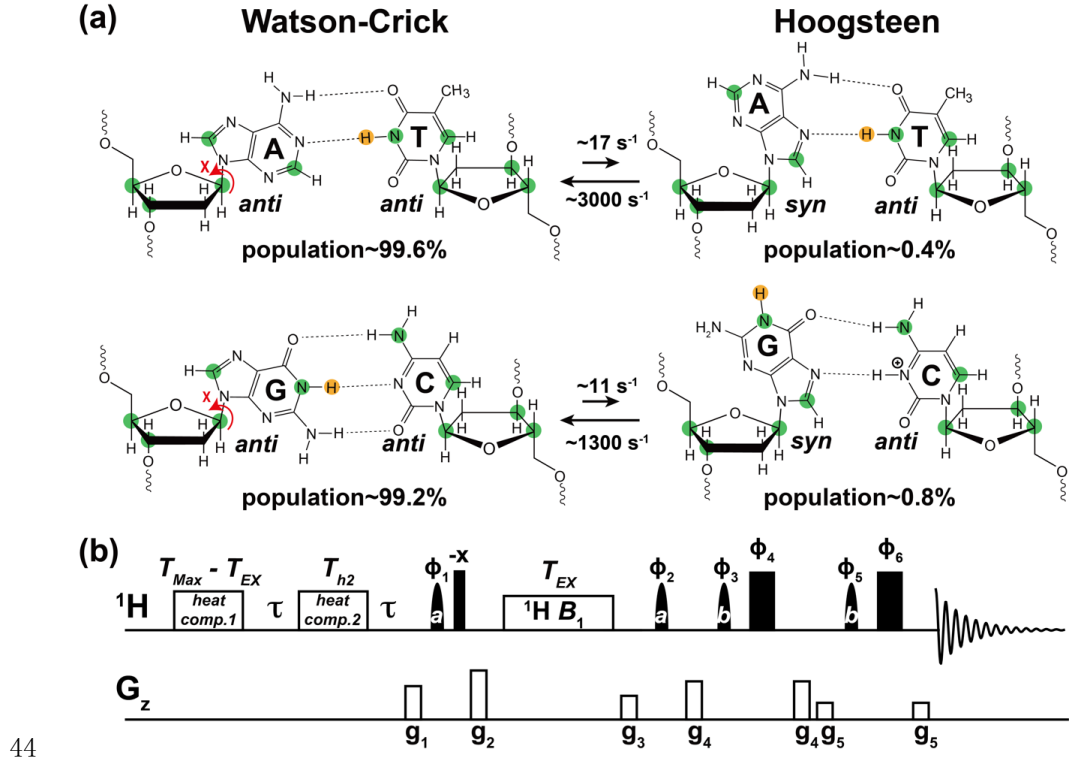

Figure 1. Using ^{1}H CEST to measure Watson-Crick to Hoogsteen exchange in unlabeled nucleic acid duplexes. (a) Watson-Crick G-C and A-T bps in B-DNA exist in dynamic equilibrium with G-C^{+} and A-T Hoogsteen bps, respectively. Filled green circles denote nuclei (^{13}C and ^{15}N) that have previously been used to probe the Watson-Crick to Hoogsteen exchange via RD measurements, while the yellow circle denotes the imino ^{1}H probes used in this study. Rate constants and populations were obtained as described previously (Alvey et al., 2014). (b) The 1D SELOPE ^{1}H CEST pulse sequence for characterizing chemical exchange in unlabeled nucleic acids. Narrow and wide filled rectangles denote 90° and 180°

https://doi.org/10.5194/mr-2021-58
Preprint. Discussion started: 20 July 2021


Open Access MAGNETIC RESONANCE Discussions

hard pulses. Semi-oval shapes denote selective pulses. Pulse **a** is a 90° Eburp2.1000 shape pulse (typically 4 ms) for selective excitation of imino protons, while pulse **b** is a 180° Squa100.1000 shape pulse with length 2 ms in an excitation sculpting scheme (Hwang and Shaka, 1995) for water suppression. Open rectangles denote the gradients and heat compensation elements. Delay τ = ½ d_1. To ensure uniform heating for experiments with variable lengths of T_{EX}, the relaxation period during which a ^{1}H B_1 field is applied, two heat compensation modules were used according to a prior study (Schlagnitweit et al., 2018). The first heat compensation is applied far off-resonance with duration = T_{Max} - T_{EX} = 2 ms, where T_{Max} is the maximum relaxation delay time. The second heat compensation (1 kHz) applied far off-resonance has a duration T_{h2} = 150 ms. The phase cycles used are ϕ_1 = {8x, 8(-x)}, ϕ_2 = {4x, 4(-x)}, ϕ_3 = {x, y}, ϕ_4 = {-x, -y}, ϕ_5 = {2x, 2y}, and ϕ_6 = {2(-x), 2(-y)}. Gradients (g1 - g5) with SMSQ10.100 profiles are applied for 1 ms with the following amplitudes (G cm^{-1}): 14.445, 26.215, 14.445, 16.585, 5.885. Briefly, imino ^{1}H magnetization is selectively excited, aligned longitudinally and then relaxes under a ^{1}H B_1 field during T_{EX}. ^{1}H transverse magnetization is then created and directly detected following water suppression. This pulse sequence is adapted from Schlagnitweit *et al* (Schlagnitweit et al., 2018).

https://doi.org/10.5194/mr-2021-58
Preprint. Discussion started: 20 July 2021


Open Access MAGNETIC RESONANCE Discussions

Following their discovery, Hoogsteen bps were observed in crystal structures of duplex DNA in complex with proteins (Kitayner et al., 2010; Aishima et al., 2002) and drugs (Wang et al., 1984; Ughetto et al., 1985) and shown to play roles in DNA recognition (Golovenko et al., 2018) , damage induction (Xu et al., 2020), and repair (Lu et al., 2010), and in damage bypass during replication (Nair et al., 2006; Ling et al., 2003). NMR relaxation dispersion (RD) studies employing off-resonance ^{13}C and ^{15}N spin relaxation in the rotating frame ($R_{1\rho}$) later showed that the G-C and A-T Watson-Crick bps exist in a dynamic equilibrium with their Hoogsteen counterparts (Nikolova et al., 2011). The Hoogsteen bps were shown to be lowly populated (population < 1 %) and short-lived (lifetime ~ 1 ms) forming robustly as an excited conformational state (ES) in duplex DNA across a variety of sequence contexts (Alvey et al., 2014) (Fig. 1a).

There is growing interest in mapping the Watson-Crick to Hoogsteen exchange landscape cross different DNA contexts, including for bps in different sequence motifs (Alvey et al., 2014), near sites of damage and mismatches (Shi et al., 2021; Singh et al., 1993), and when DNA is bound to proteins (Nikolova et al., 2013b; Zhou et al., 2019) and drugs (Xu et al., 2018; Wang et al., 1984). Studies suggest an increased propensity to form Hoogsteen bps in such environments (Shi et al., 2021) and this may in turn play roles in DNA recognition and damage repair (Afek

https://doi.org/10.5194/mr-2021-58
Preprint. Discussion started: 20 July 2021


Open Access MAGNETIC RESONANCE Discussions

et al., 2020). Furthermore, there is interest in understanding how the Hoogsteen exchange varies with temperature (Nikolova et al., 2011), pH (Nikolova et al., 2013a), salt concentration and buffer composition (Rangadurai et al., 2020b; Tateishi-Karimata et al., 2014), as well as in the presence of epigenetic modifications (Wang et al., 2017; Rangadurai et al., 2019a), all of which could shape these dynamics and consequently DNA biochemical transactions.

There are hundreds and thousands of motifs and conditions for which characterization of Hoogsteen dynamics is of biological interest. However, current approaches for measuring Hoogsteen dynamics are ill-suited for dynamics measurements at such a scale. The Watson-Crick to Hoogsteen chemical exchange process has been characterized with the use of ^{13}C (Nikolova et al., 2011; Shi et al., 2018; Ben Imeddourene et al., 2020; Alvey et al., 2014) and ^{15}N (Nikolova et al., 2012a; Rangadurai et al., 2019a; Alvey et al., 2014) off-resonance $R_{1\rho}$, and more recently chemical exchange saturation transfer (CEST) experiments (Rangadurai et al., 2020b; Rangadurai et al., 2020a). However, these approaches require isotopically enriched DNA samples, making broad explorations of Hoogsteen exchange across even tens of motifs impractical. Furthermore, many motifs of interest involve damaged or modified nucleotides, which are difficult to isotopically enrich with ^{13}C and ^{15}N nuclei. It is for this reason that we turned our

https://doi.org/10.5194/mr-2021-58
Preprint. Discussion started: 20 July 2021


Open Access MAGNETIC RESONANCE Discussions

attention to the imino ^{1}H as a probe of the Watson-Crick to Hoogsteen exchange in unlabeled DNA samples.

The utility of protons as probes in CEST (Chen et al., 2016; Dubini et al., 2020; Wang et al., 2021; Liu et al., 2020), Carr-Purcell-Meiboom-Gill (CPMG) (Juen et al., 2016; Leblanc et al., 2018), and off-resonance $R_{1\rho}$ experiments (Wang and Ikuta, 1989; Lane et al., 1993; Steiner et al., 2016; Schlagnitweit et al., 2018; Baronti et al., 2020; Furukawa et al., 2021) to study conformational exchange in nucleic acids is now well-established. Many of these ^{1}H based approaches use experiments originally developed to study conformational exchange in proteins (Ishima et al., 1998; Eichmuller and Skrynnikov, 2005; Lundstrom and Akke, 2005; Lundstrom et al., 2009; Otten et al., 2010; Bouvignies and Kay, 2012; Hansen et al., 2012; Weininger et al., 2012; Weininger et al., 2013; Smith et al., 2015; Sekhar et al., 2016; Yuwen et al., 2017a; Yuwen et al., 2017b). The ^{1}H experiments permit the use of higher effective fields allowing characterization of conformational exchange faster than is possible using ^{13}C or ^{15}N experiments (Steiner et al., 2016; Palmer, 2014). Furthermore, the relationship between ^{1}H chemical shifts and structure is reasonably well understood and has been exploited in the conformational characterization of nucleic acids (Sripakdeevong et al., 2014;

https://doi.org/10.5194/mr-2021-58
Preprint. Discussion started: 20 July 2021


Open Access MAGNETIC RESONANCE Discussions

133 Frank et al., 2013; Wang et al., 2021; Swails et al., 2015; Czernek et al., 2000;
134 Lam and Chi, 2010).
135
136 Recently, ^{1}H $R_{1\rho}$ and CEST SELective Optimized Proton Experiments (SELOPE)
137 were developed and applied to characterize conformational exchange in unlabeled
138 RNA (Schlagnitweit et al., 2018). The SELOPE experiment has already found
139 several applications in studies of unlabeled nucleic acids, including in the
140 characterization of fast (k_{ex} = k_1 + k_{-1} > 1,000 s^{-1}) RNA secondary structural
141 rearrangements (Baronti et al., 2020) and DNA base opening (Furukawa et al.,
142 2021), as well as slower (k_{ex} < 100 s^{-1}) DNA hybridization kinetics (Dubini et al.,
143 2020). Many ^{1}H relaxation dispersion (RD) studies have targeted exchangeable
144 imino protons (Baronti et al., 2020; Furukawa et al., 2021), taking advantage of the
145 well-known dependence of the imino ^{1}H chemical shifts on secondary structure
146 (Wang et al., 2021; Lam and Chi, 2010).
147
148 Although ^{1}H RD experiments can obviate the need for isotopic labeling and offer
149 other advantages such as high sensitivity, they have not been as widely used
150 compared to ^{13}C/^{15}N RD experiments. One reason for this has to do with potential
151 artifacts arising due to from ^{1}H-^{1}H cross relaxation (Ishima et al., 1998; Eichmuller
152 and Skrynnikov, 2005; Lundstrom and Akke, 2005; Bouvignies and Kay, 2012).

https://doi.org/10.5194/mr-2021-58
Preprint. Discussion started: 20 July 2021


Open Access MAGNETIC RESONANCE Discussions

153 Interestingly, in nucleic acids, such NOE effects appear to be effectively
154 suppressed in the ^{1}H SELOPE experiment through selective excitation of spins
155 (Schlagnitweit et al., 2018). The exchange parameters obtained using ^{1}H SELOPE
156 experiments were shown to be in very good agreement with counterparts obtained
157 using ^{13}C and ^{15}N off-resonance $R_{1\rho}$ (Baronti et al., 2020). In addition, similar
158 exchange parameters were obtained when using variable tilt angles in $R_{1\rho}$
159 experiments, including tilt angle of 35.3° in which ROE and NOE cross-relaxation
160 terms cancel (Eichmuller and Skrynnikov, 2005; Weininger et al., 2013; Steiner et
161 al., 2016). No NOE dips or artifacts were observed in the majority of the ^{1}H CEST
162 or off-resonance $R_{1\rho}$ profiles (Steiner et al., 2016; Dubini et al., 2020; Furukawa et
163 al., 2021). These results are consistent with a prior off-resonance ^{1}H $R_{1\rho}$ studies
164 showing that even without deuteration, it is feasible to effectively suppress cross-
165 relaxation between amide and aliphatic protons through selective inversion of
166 amide protons and use of short spin lock relaxation delays (Lundstrom and Akke,
167 2005; Schlagnitweit et al., 2018). Nevertheless, NOE effects have been reported
168 for select sites in ^{1}H SELOPE studies of nucleic acids (Schlagnitweit et al., 2018),
169 and in ^{1}H CEST studies of proteins (Bouvignies and Kay, 2012; Sekhar et al., 2016;
170 Yuwen et al., 2017a; Yuwen et al., 2017b). This underscores the need to carefully
171 analyze NOE effects, especially for unlabeled samples, in which spin-state-

https://doi.org/10.5194/mr-2021-58
Preprint. Discussion started: 20 July 2021


Open Access MAGNETIC RESONANCE Discussions

172 selective magnetization transfer schemes (Yuwen et al., 2017a; Yuwen et al.,
173 2017b) employing heteronuclei to suppress NOE effects are not feasible.
174
175 There are certain conditions in which the Hoogsteen bp becomes the dominant
176 conformation in duplex DNA. These include chemically modified bases (Nikolova
177 et al., 2011), when DNA is in complex with binding partners (Xu et al., 2018), and
178 for specific sequence contexts under certain experimental conditions (Stelling et
179 al., 2017). Based on NMR studies of such duplexes containing Hoogsteen bps,
180 there should be a sizeable difference (Δω ~-1 – -2 ppm) between the imino proton
181 chemical shifts of guanine (G-H1) and thymine (T-H3) in the Hoogsteen versus
182 Watson-Crick conformation. These differences should render G-H1 and T-H3
183 suitable probes of Hoogsteen exchange in unlabeled DNA duplexes provided that
184 NOE effects can be effectively suppressed. Imino protons are also attractive
185 probes given that they are often well-resolved even in 1D ^{1}H spectra of large RNAs.
186
187 Here, we show that high power ^{1}H CEST SELOPE experiments targeting the imino
188 protons G-H1 and T-H3 provide facile means for measuring Watson-Crick to
189 Hoogsteen exchange of G-C and A-T bps in DNA without the need for isotopic
190 enrichment. NOE effects are shown to have a negligible contribution as short
191 (≤100 ms) relaxation delays can be used to characterize the relatively fast (k_{ex} ~

https://doi.org/10.5194/mr-2021-58
Preprint. Discussion started: 20 July 2021


Open Access MAGNETIC RESONANCE Discussions

500 to 8,000 s^{-1}) Watson-Crick to Hoogsten exchange process (Alvey et al., 2014). The approach also takes advantage of high-power radio-frequency (RF) fields recently shown (Rangadurai et al., 2020a) to extend the timescale sensitivity of CEST to include faster exchange processes that traditionally are more effectively characterized with the use of $R_{1\rho}$. The high-power ^{1}H CEST experiment also enabled measurement of fast Hoogsteen exchange kinetics (k_{ex} > 20,000 s^{-1}) inaccessible to conventional ^{13}C or ^{15}N off-resonance $R_{1\rho}$ RD. The ^{1}H CEST experiment opens the door to more comprehensively and systematically exploring how the Watson-Crick to Hoogsteen exchange process varies with sequence and structural contexts, and physiological conditions of interest.

https://doi.org/10.5194/mr-2021-58
Preprint. Discussion started: 20 July 2021


Open Access MAGNETIC RESONANCE Discussions

203 ## 2 Results

204 ### 2.1 Assessment of NOE effects

205 We used the SELOPE (Schlagnitweit et al., 2018) experiment (Fig. 1b) to measure
206 ^{1}H CEST profiles for G-H1 and T-H3 in unlabeled DNA duplexes (Fig. 2) at 25 °C-
207 26 °C. We used ^{1}H CEST rather than $R_{1\rho}$ given the greater ease of collecting
208 profiles for many spins simultaneously, and given that with the use of high-power
209 RF fields, CEST can effectively characterize exchange processes over a wide
210 range of timescales (Rangadurai et al., 2020a). Use of high power RF fields was
211 recently shown to be important to effectively characterize the comparatively fast
212 (k_{ex} ~ 3,000 s^{-1}) Watson-Crick to Hoogsteen exchange process using ^{13}C and ^{15}N
213 CEST experiments (Rangadurai et al., 2020a). Here, we also employed high
214 power RF fields (> 250 Hz) to optimally characterize Watson-Crick to Hoogsteen
215 exchange using ^{1}H CEST.
216

https://doi.org/10.5194/mr-2021-58
Preprint. Discussion started: 20 July 2021

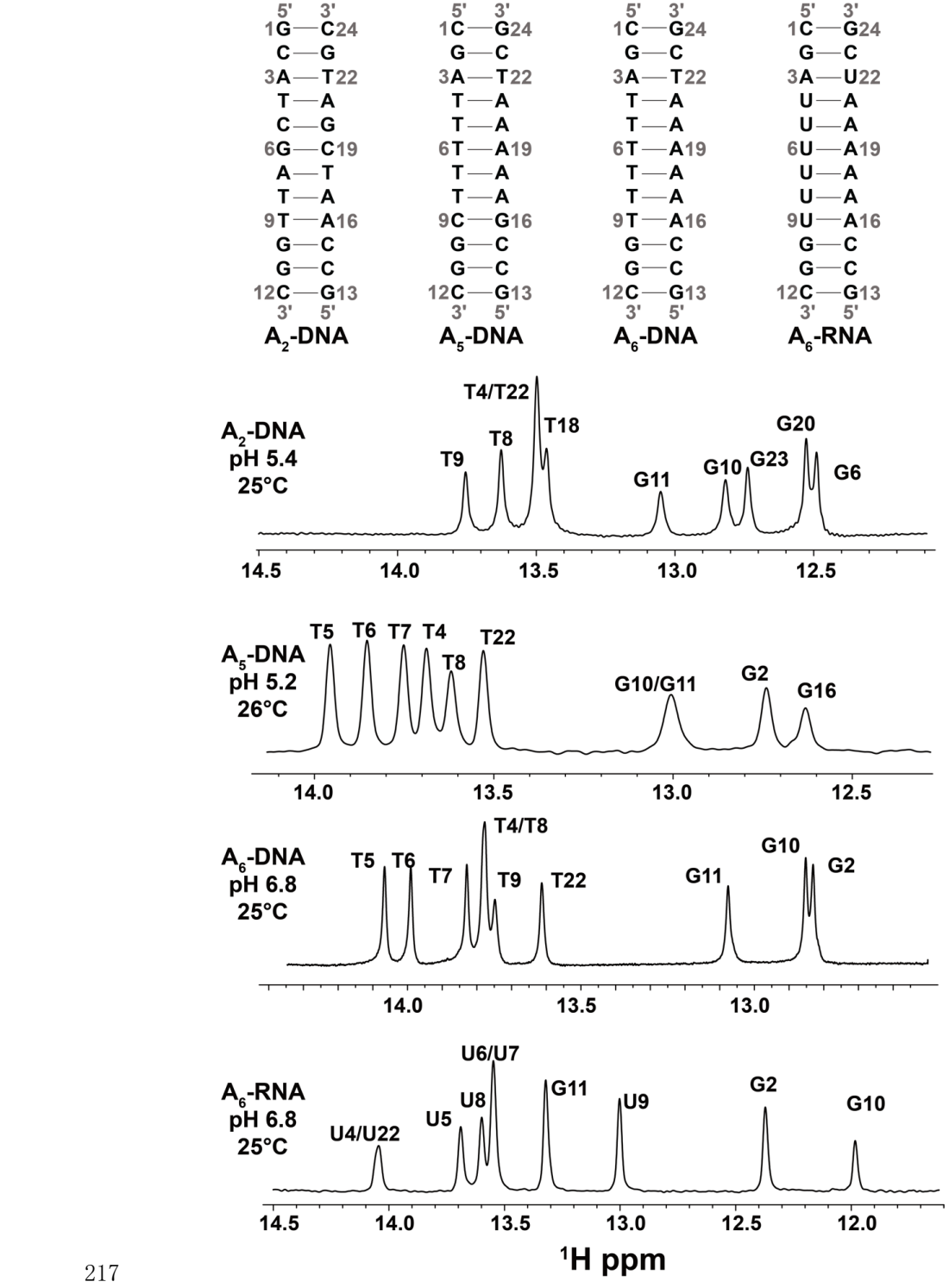

217

https://doi.org/10.5194/mr-2021-58
Preprint. Discussion started: 20 July 2021


Open Access MAGNETIC RESONANCE Discussions

Figure 2. DNA and RNA duplexes used in this study. Also shown are 1D ^{1}H spectra of the imino region. The buffer conditions were 25 mM sodium chloride, 15 mM sodium phosphate, 0.1 mM EDTA and 10 % D_2O. The pH and temperature are indicated on each spectrum.

An important consideration when performing ^{1}H CEST experiments are contributions due to ^{1}H-^{1}H cross-relaxation, which may give rise to extraneous NOE dips in the ^{1}H CEST profiles (Ishima et al., 1998; Lundstrom and Akke, 2005; Eichmuller and Skrynnikov, 2005; Bouvignies and Kay, 2012; Sekhar et al., 2016; Yuwen et al., 2017a; Yuwen et al., 2017b). These contributions have been suppressed in proteins through deuteration (Eichmuller and Skrynnikov, 2005; Lundstrom and Akke, 2005; Lundstrom et al., 2009; Otten et al., 2010; Hansen et al., 2012; Weininger et al., 2012), and in ^{15}N isotopically labelled proteins (Yuwen et al., 2017a; Yuwen et al., 2017b) and nucleic acids (Wang et al., 2021; Liu et al., 2020) using spin-state-selective magnetization transfer schemes, and through selective inversion of protons combined with use of short relaxation times (Lundstrom and Akke, 2005; Schlagnitweit et al., 2018).

https://doi.org/10.5194/mr-2021-58
Preprint. Discussion started: 20 July 2021


Open Access MAGNETIC RESONANCE Discussions

237 In the SELOPE experiment, imino protons are selectively excited and the
238 magnetization belonging to non-imino protons is dephased prior to application of
239 the B_1 field. This helps to suppress cross-relaxation (Yamazaki et al., 1994)
240 between the imino and non-imino protons (*vide infra*). In addition, because the
241 Watson-Crick to Hoogsteen exchange is relatively fast with k_{ex} = ~500 – 8000 s^{-1}
242 at 25 °C (Alvey et al., 2014), we could afford to use a relatively short relaxation
243 delay of 100 ms which also helped minimize NOE effects (*vide infra*) (Lundstrom
244 and Akke, 2005; Schlagnitweit et al., 2018).
245
246 We initially performed experiments to evaluate contributions from ^{1}H-^{1}H cross-
247 relaxation to the imino ^{1}H CEST profiles. In canonical B-form DNA and A-form
248 RNA duplexes (Fig. 2), G-H1 is in closest proximity to the partner base C-H4a
249 (~2.4 Å, Fig. 3a), while T/U-H3 is in closest proximity to the partner A-H2 (~2.8 Å,
250 Fig. 3a). Additional proximal protons include imino and H2 protons of neighboring
251 residues (~3.5-3.6 Å, Fig. 3a). These short internuclear distances are reflected in
252 the intensity of cross peaks in 2D [^{1}H, ^{1}H] NOESY spectra of nucleic acid duplexes
253 (Fig. 3b and Fig. S1). Note that although the amino proton of G-H2a is in proximity
254 (2.2 Å) to G-H1, while the amino proton of A-H6a is in proximity (2.4 Å) to the
255 partner T-H3 (Fig. 3a), these amino protons are typically not observable in 1D ^{1}H

https://doi.org/10.5194/mr-2021-58
Preprint. Discussion started: 20 July 2021

Open Access MAGNETIC RESONANCE Discussions

256 or 2D [^{1}H,^{1}H] NOESY spectra caused by intermediate exchange due to the
257 restricted rotation around the C-NH_2 bond (Schnieders et al., 2019).
258

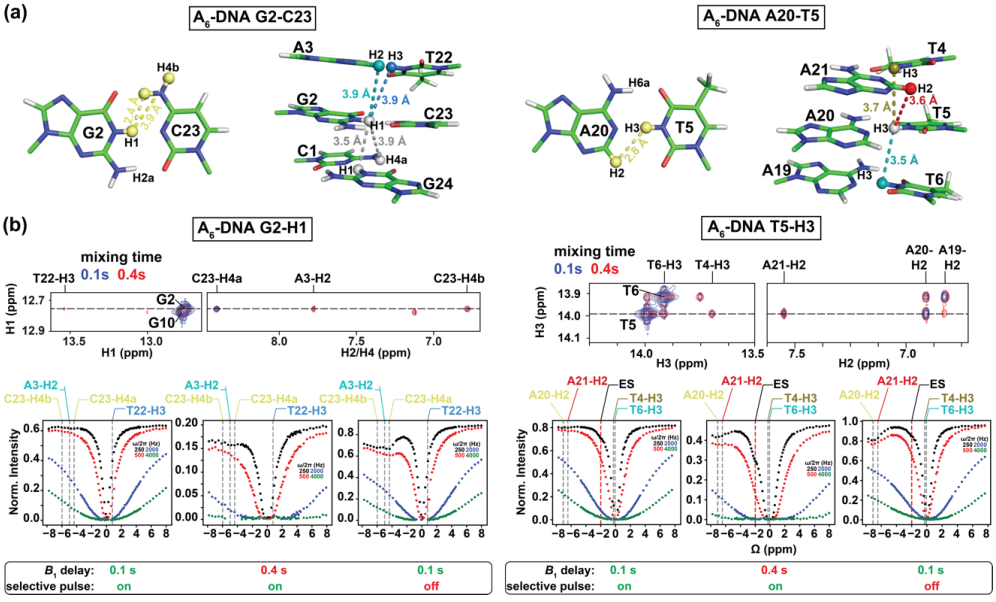

259

260 **Figure 3. Analyzing NOE effects in ^{1}H CEST profiles.** (a) Distances between
261 the imino protons of G2-H1 and T5-H3 and nearby protons in the A_6-DNA duplex
262 (PDBID: 5UZF). Note that although the amino proton of G-H2a is in proximity (2.2
263 Å) to G-H1, while the amino proton of A-H6a is in proximity (2.4 Å) to the partner
264 T-H3, these amino protons are not observable in 1D ^{1}H or 2D [^{1}H,^{1}H] NOESY
265 spectra caused by intermediate exchange due to the restricted rotation around the
266 C-NH_2 bond (Schnieders et al., 2019). (b) NOE dips in ^{1}H CEST profiles for G2-
267 H1 and T5-H3 in A_6-DNA. The NOE diagonal and cross peaks for G2-H and T5-

https://doi.org/10.5194/mr-2021-58
Preprint. Discussion started: 20 July 2021


Open Access MAGNETIC RESONANCE Discussions

268 H3 in the 2D [^{1}H, ^{1}H] NOESY spectra with mixing time 100 ms (blue) and 400 ms
269 (red) are shown on the top. The ^{1}H CEST profiles for G2-H1 and T5-H3 with
270 combinations of short (100 ms) and long (400 ms) relaxation delays, with and
271 without selective excitation (Methods) are shown at the bottom. The ES frequency
272 (black) obtained from fitting ^{1}H CEST profiles with selective excitation and short
273 relaxation delay (100 ms) as well as frequency positions corresponding to the NOE
274 cross peaks in the 2D [^{1}H, ^{1}H] NOESY spectra (top) are highlighted according to
275 the color scheme in (a) (bottom). Error bars for CEST profiles in (b), which are
276 smaller than the data points, were obtained using triplicate experiments, as
277 described in Methods. RF powers for CEST profiles are color-coded.
278
279
280 ^{1}H CEST profiles (Fig. 3b and Fig. S2) for well-resolved imino resonances of A_6-
281 DNA (Fig. 2) were acquired simultaneously in a 1D manner using ~3 hours of
282 acquisition time on a spectrometer operating at 600 MHz ^{1}H frequency equipped
283 with a cryogenic probe, and using ~1.0 mM unlabeled DNA (Methods). Data were
284 initially collected at pH = 6.8. Under these near neutral pH conditions, it is
285 generally not feasible to detect the Watson-Crick to Hoogsteen exchange process
286 for G-C bps due to the low population of the protonated G-C$^+$ Hoogsteen bp
287 (Nikolova et al., 2013a). The lack of expected dips for the ES G-C$^+$ Hoogsteen bp

https://doi.org/10.5194/mr-2021-58
Preprint. Discussion started: 20 July 2021


Open Access MAGNETIC RESONANCE Discussions

288 under these conditions provides an opportunity to better assess any extraneous
289 ^{1}H CEST dips arising due to NOE effects. Unlike for G-C bps, the Hoogsteen
290 exchange should still be detectable for A-T bps under these pH conditions.
291
292 Shown in Fig. 3b is a representative imino ^{1}H CEST profile measured for G2-H1 in
293 the well-characterized A_6-DNA duplex (Nikolova et al., 2011). Besides the major
294 dip, no additional dips were visible in the ^{1}H CEST profile. The major dip was also
295 symmetric (Rangadurai et al., 2020a), indicating little to no contribution from
296 Hoogsteen exchange or NOE effects, as expected for G-C bps under these pH
297 conditions (Nikolova et al., 2013a). On the other hand, a minor shoulder was
298 observed in the ^{1}H CEST profile of T5-H3 (Fig. 3b). The shoulder occurs at an
299 offset frequency that does not correspond with any other observable proton
300 frequency in the A_6-DNA duplex and is therefore unlikely to be the result of NOE
301 effects (Fig. 3a). Rather, as will be described below, the shoulder corresponds to
302 the ES Hoogsteen bp which is to be expected for the A-T bp at pH = 6.8.
303
304 To verify that the dips observed in the ^{1}H CEST profile of T5-H3 and other thymine
305 residues in A_6-DNA (see Fig. 4 and S2) do not represent an NOE effect, we
306 performed ^{1}H CEST experiments on a corresponding A_6-RNA duplex (Fig. 2).
307 Unlike in B-form DNA duplexes, G-C^{+} and A-U Hoogsteen bps are both

https://doi.org/10.5194/mr-2021-58
Preprint. Discussion started: 20 July 2021


Open Access MAGNETIC RESONANCE Discussions

undetectable in A-form RNA duplexes by off-resonance ^{13}C and ^{15}N $R_{1\rho}$ RD, most likely due their much lower population (p_{ES} < 0.04 %) (Zhou et al., 2016; Rangadurai et al., 2018). If the shoulder observed in the ^{1}H CEST profile of T5-H3 in A_6-DNA is due to a Hoogsteen ES, and not NOE dips, we would expect to observe a symmetric profile without ES dips for U5-H3 in A_6-RNA. Indeed, the corresponding ^{1}H CEST profiles for U5-H3 (Fig. 4) and all other uridine and guanine (Fig. S3) imino protons in A_6-RNA were symmetric, with no evidence for any asymmetry or shoulder, indicating the absence of exchange and NOE effects.

https://doi.org/10.5194/mr-2021-58
Preprint. Discussion started: 20 July 2021

Open Access MAGNETIC RESONANCE Discussions

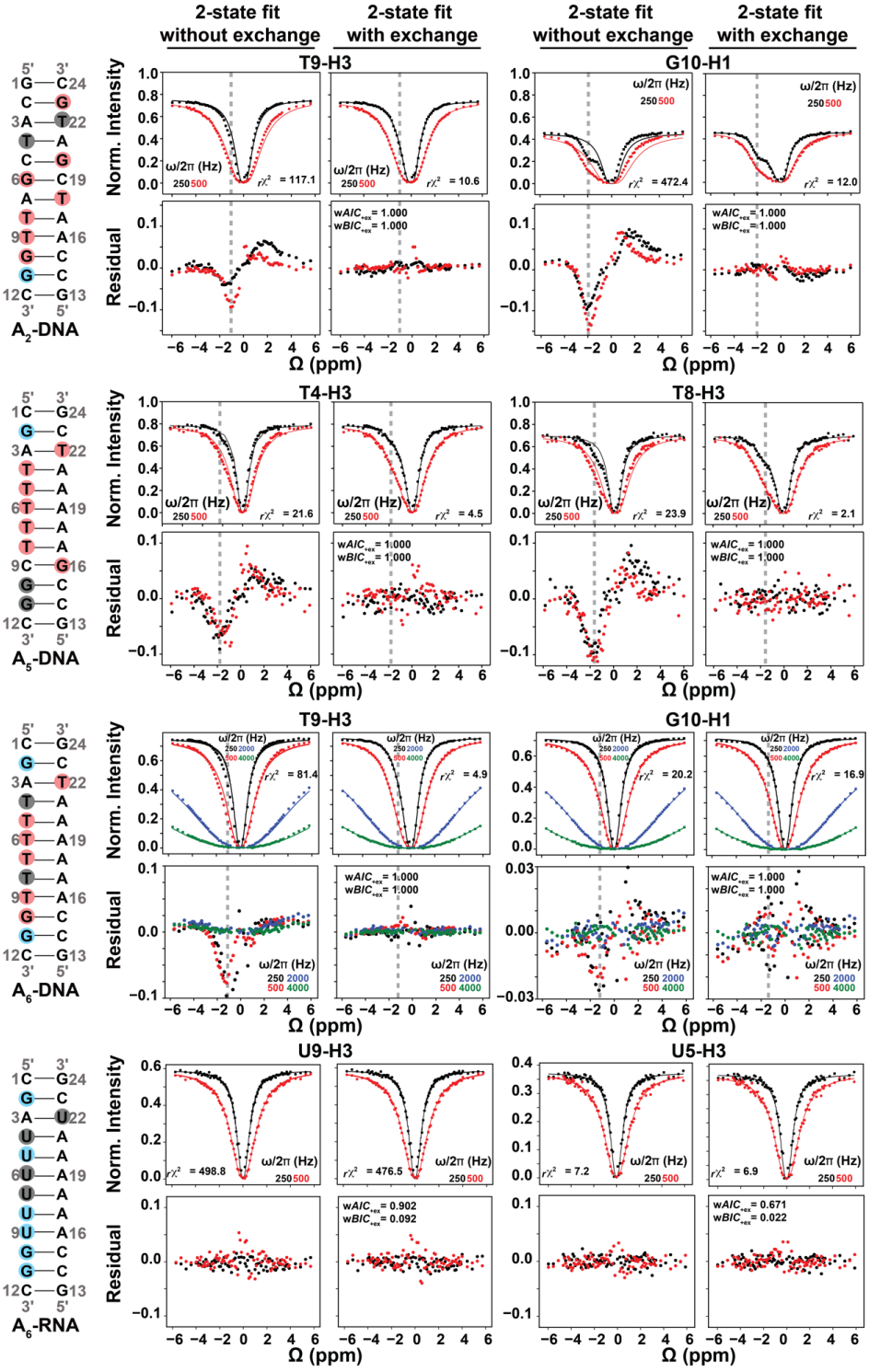

317

https://doi.org/10.5194/mr-2021-58
Preprint. Discussion started: 20 July 2021


Open Access MAGNETIC RESONANCE Discussions

318 **Figure 4.** Representative ^{1}H CEST profiles measured for A_2-DNA (pH 5.4) at 25
319 °C, A_5-DNA (pH 5.2) at 26 °C, A_6-DNA (pH 6.8) at 25 °C and A_6-RNA (pH 6.8) at
320 25 °C. Residues with detectable RD, undetectable RD, and overlapped 1D ^{1}H
321 resonances (see Fig. 2) are highlighted in red, blue, and gray circles respectively.
322 Shown are the fits of the ^{1}H CEST data to a 2-state Bloch-McConnell equation with
323 and without (k_{ex} = Δω = p_{ES} = 0) chemical exchange. Shown below the CEST
324 profiles are residual (experimental normalized intensity - fitted normalized
325 intensity) plots. Also shown in inset are the reduced chi-square ($r\chi^2$), and Akaike's
326 (w*AIC*) and Bayesian information criterion (w*BIC*) weights for fits with exchange
327 (Methods). The dashed gray lines indicate the Hoogsteen Δω positions in both ^{1}H
328 CEST profiles and in residual plots. Error bars for CEST profiles, which are smaller
329 than the data points, were obtained using triplicate experiments, as described in
330 Methods. RF powers for CEST profiles are color-coded.
331
332
333 Therefore, the shoulders in the ^{1}H CEST profiles (Fig. 3,4, Fig. S2,3) most likely
334 rise due to chemical exchange with an ES. This was further confirmed by
335 evaluating whether fits to the ^{1}H CEST profiles show any statistically significant
336 improvement with the inclusion of exchange, as described below. Based on a
337 similar analysis, no NOE dips were observable in the ^{1}H CEST profiles (Fig. 4,

https://doi.org/10.5194/mr-2021-58
Preprint. Discussion started: 20 July 2021


Open Access MAGNETIC RESONANCE Discussions

S2,3) for all other residues in A_6-DNA, A_6-RNA, and in two other DNA duplexes across a range of pH and temperature conditions when using selective excitation and relaxation delay of 100 ms (Fig. 2, Fig. 4, and S2,3). These results indicate that any NOE effects between imino and non-imino protons are small under these experimental conditions.

NOE dips arising from cross-relaxation to neighboring imino protons (Fig. 3a) are more difficult to assess, as they would be buried within the major dip (Fig. 3b). However, since no NOE dips were observable for non-imino protons within 2.8 Å (Fig. 3a), a sizeable cross-relaxation contribution from neighboring imino protons is unlikely considering they are separated by a longer internuclear distance of ~3.7-3.9 Å (Fig. 3a), and correspondingly, have weaker intensities in 2D NOESY spectra (Fig. 3b). Nevertheless, whether or not these NOE effects are large enough to impact determination of the exchange parameters was examined (*vida infra*) through comparison of the exchange parameters derived from fitting the imino ^{1}H CEST profiles with those measured independently using off-resonance ^{13}C and ^{15}N $R_{1\rho}$ RD measurements.

Importantly, upon increasing the relaxation delay to 400 ms, or using a non-selective ^{1}H excitation pulse (pulse **a** in Fig. 1b) with a delay of 100 ms, NOE dips

https://doi.org/10.5194/mr-2021-58
Preprint. Discussion started: 20 July 2021


Open Access MAGNETIC RESONANCE Discussions

358 became visible in the ^{1}H CEST profiles as shown for G2-H1 and T5-H3 (Fig. 3b)
359 in A_6-DNA. The dips occurred at the ^{1}H resonance frequency of nearby protons,
360 and as expected, were particularly pronounced for the partner C-H4a in the case
361 of G2-H1 and the partner A-H2 in the case of T5-H3 (Fig. 3b). Nevertheless, the
362 ^{1}H CEST profiles acquired with 400 ms delay could be fit when restricting the offset
363 to the imino proton region (-3 - 3 ppm), and the fitted exchange parameters were
364 similar to those obtained from fitting profiles with 100 ms relaxation delay in which
365 no NOE dips were visible (Fig. S4, Table S1). In contrast, the ^{1}H CEST profiles
366 measured using non-selective excitation, which had larger NOE dips relative to
367 using a selective excitation pulse, could not be satisfactorily fit (Fig. S4). These
368 results underscore the importance of critically evaluating the NOE contributions on
369 a case-by-case basis (Schlagnitweit et al., 2018) and also suggest that NOE
370 effects can be effectively suppressed for the canonical duplexes used in this study
371 provided use of selective excitation and short relaxation delays.
372
373 It should be noted that to avoid any complexities due to NOE effects with water
374 protons or hydrogen exchange, we restricted the offset to -6 ppm – 6 ppm when
375 analyzing and fitting the ^{1}H CEST profiles. This is common practice as relatively
376 narrow offsets (< 4 ppm) were used in prior ^{1}H CEST studies of both nucleic acids
377 (Dubini et al., 2020; Wang et al., 2021; Liu et al., 2020) and proteins (Yuwen et al.,

https://doi.org/10.5194/mr-2021-58
Preprint. Discussion started: 20 July 2021


Open Access MAGNETIC RESONANCE Discussions

2017a; Yuwen et al., 2017b). While we did not observe a dip near the water chemical shift in the ^{1}H CEST profile for the internal residue T5-H3, a weak and broad dip near the water chemical shift was observed in the profile for the near terminal residue G2-H1 (Fig. S2). The latter dip could be due to NOEs between G2-H1 and water protons and/or due to fast hydrogen exchange kinetics.

2.2 Benchmarking the utility of ^{1}H CEST to probe Watson-Crick to Hoogsteen exchange in DNA duplexes

To examine the utility of the SELOPE ^{1}H CEST experiment to characterize Watson-Crick to Hoogsteen exchange, we benchmarked the experiment by measuring conformational exchange in three DNA duplexes (A_6-DNA, A_2-DNA and A_5-DNA, Fig. 2) for which we have previously extensively characterized the Watson-Crick to Hoogsteen exchange using ^{13}C and ^{15}N off-resonance $R_{1\rho}$ (Nikolova et al., 2011; Alvey et al., 2014; Shi et al., 2018) and CEST (Rangadurai et al., 2020a; Rangadurai et al., 2020b) experiments. We compared the exchange parameters derived using ^{1}H CEST with counterparts derived using ^{13}C/^{15}N $R_{1\rho}$ or CEST for a variety of G-C and A-T bps across three different DNA duplexes and varying pH (5.2-6.8) conditions. All ^{1}H CEST experiments were performed using 100 ms relaxation delay and selective excitation.

https://doi.org/10.5194/mr-2021-58
Preprint. Discussion started: 20 July 2021


Open Access MAGNETIC RESONANCE Discussions

As expected, for several thymine residues, the imino ^{1}H CEST profile was visibly asymmetric (Fig. 4 and Fig. S2,3), consistent with relatively fast (k_{ex} > 1000 s^{-1}) Watson-Crick to Hoogsteen exchange. The asymmetry manifests as an upfield shifted shoulder (e.g. T8-H3 in A_5-DNA in Fig. 4) as expected for T-H3 Hoogsteen chemical shift (Δω ~-2 ppm) (Nikolova et al., 2011; Xu et al., 2018). In other cases, such as T9-H3 in A_6-DNA, the asymmetry was less pronounced, and the exchange contribution was only apparent following comparison of fits with and without exchange (see Fig. 4).

As expected, at pH = 6.8, the imino ^{1}H CEST profiles were symmetric for most guanine residues consistent with no observable exchange (Fig. 4 and S2,3). However, the major dip became asymmetric for several guanine residues when lowering the pH to 5.2 or 5.4, as expected for the Watson-Crick to Hoogsteen exchange of G-C bps, which is favored at lower pH (Fig. 4 and S3). All minor dips occurred at resonance frequencies that did not correspond with any other protons in the molecule (Fig. 2 and S1,2). In all cases, the ^{1}H CEST profiles could be satisfactorily fit to a 2-state model with or without exchange, suggesting that any NOE contribution to the ^{1}H CEST profile is likely to be insignificant.

https://doi.org/10.5194/mr-2021-58
Preprint. Discussion started: 20 July 2021


Open Access MAGNETIC RESONANCE Discussions

To identify which imino ^{1}H CEST profiles have significant chemical exchange contributions, each profile was subjected to a fit with or without ($\Delta\omega = p_{ES} = k_{ex} = 0$) 2-state chemical exchange (Methods). Akaike information criterion (AIC) and Bayesian information criterion (BIC) (Burnham and Anderson, 2004) weights were then used to evaluate whether any improvement in the fit due to inclusion of chemical exchange was statistically significant (Kimsey et al., 2018; Liu et al., 2020). The improvement of fit was considered to be statistically significant when both AIC and BIC weights > 0.995 and the reduced chi-square ($r\chi^2$) is reduced with the inclusion of exchange. Residual plots were also used to visualize changes in fit quality (Fig. 4).

Based on the AIC and BIC analysis, all thymine and guanine residues shown previously to undergo Watson-Crick to Hoogsteen exchange using off-resonance ^{13}C and/or ^{15}N $R_{1\rho}$ under these experimental conditions, also showed statistically significant improvements when fitting the ^{1}H CEST profiles with the inclusion of chemical exchange (Fig. 4 and S2,3). On the other hand, all guanine residues including G2 and G11 in A_6-DNA and G11 in A_2-DNA, which did not show signs of Hoogsteen exchange in off-resonance ^{13}C and/or ^{15}N $R_{1\rho}$ (Nikolova et al., 2011; Shi et al., 2018) under these experimental conditions also did not show statistically

https://doi.org/10.5194/mr-2021-58
Preprint. Discussion started: 20 July 2021


Open Access MAGNETIC RESONANCE Discussions

436 significant improvements when fitting their ^{1}H CEST profiles with the inclusion of
437 chemical exchange (Fig. 4 and S2,3).
438
439 Interestingly, a few residues including T5, T6, T7 and T22 in A_6-DNA, T18, G6 and
440 G20 in A_2-DNA (Fig. S2,3), showed exchange based on ^{1}H CEST but did not show
441 evidence for Hoogsteen exchange based on prior off-resonance ^{13}C and/or ^{15}N $R_{1\rho}$
442 experiments (Nikolova et al., 2011; Alvey et al., 2014; Shi et al., 2018). As will be
443 elaborated in the following section, these data provide new insights into the
444 Watson-Crick to Hoogsteen exchange process, and suggest that at least in some
445 cases, ^{1}H CEST can exceed the detection limits of ^{13}C/^{15}N based methods.
446
447 In addition, T18 and G20 in A_2-DNA were difficult to probe using ^{13}C RD due to
448 spectra overlap (Nikolova et al., 2011) but could easily be measured using ^{1}H
449 CEST (Fig. 2, 4 and S3). In contrast, other residues such as T8 and T4 in A_6-DNA,
450 T4 and T22 in A_2-DNA, and G10 and G11 in A_5-DNA could be targeted for ^{13}C or
451 ^{15}N RD measurements (Nikolova et al., 2011; Alvey et al., 2014) but could not be
452 measured by ^{1}H CEST due to overlap in the 1D ^{1}H imino spectra (Fig. 2). This
453 highlights the complementarity of ^{1}H and ^{13}C/^{15}N RD in characterizing Watson-
454 Crick to Hoogsteen exchange.
455

https://doi.org/10.5194/mr-2021-58
Preprint. Discussion started: 20 July 2021


Open Access MAGNETIC RESONANCE Discussions

To assess how well the exchange parameters are determined by the ^{1}H CEST data, we subjected the ^{1}H CEST profiles for residues T7 ($k_{ex}/\Delta\omega \sim 0.2$), T9 ($k_{ex}/\Delta\omega \sim 0.82$) and T22 ($k_{ex}/\Delta\omega \sim 3.5$) which exhibit exchange on the slow, intermediate, and fast timescale (Rangadurai et al., 2019b) respectively, to a degeneracy analysis. We computed the reduced chi-square ($r\chi^2$) for a 2-state fit as a function of varying k_{ex}, $\Delta\omega$ or p_{ES}. In all cases, the $r\chi^2$ values increased significantly (up to 10-fold) when varying k_{ex}, $\Delta\omega$ or p_{ES} by 3-fold (Fig. S5), indicating that the exchange parameters are well-defined by the ^{1}H CEST data.

To verify that the exchange process sensed by ^{1}H CEST does indeed correspond to Watson-Crick to Hoogsteen exchange, we compared the exchange parameters, p_{ES} and k_{ex}, derived from a 2-state fit of the data to values determined previously using off-resonance ^{13}C and/or ^{15}N $R_{1\rho}$ (Nikolova et al., 2011; Shi et al., 2018; Alvey et al., 2014) for Hoogsteen dynamics (Fig. 5a and Table S1). In total, we were able to compare 13 data points from ^{1}H CEST and ^{13}C/^{15}N $R_{1\rho}$ for three different duplexes under different conditions of temperature and pH (Fig. 2,5a).

https://doi.org/10.5194/mr-2021-58
Preprint. Discussion started: 20 July 2021

Open Access MAGNETIC RESONANCE Discussions

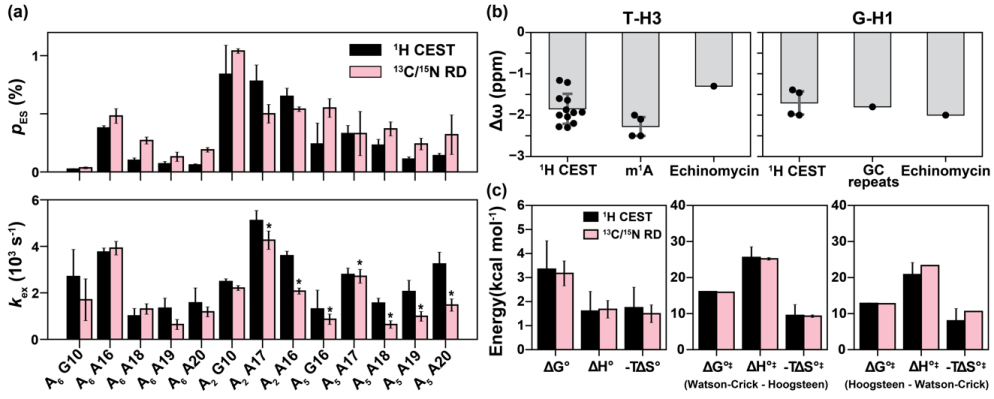

Figure 5. Comparison of exchange parameters for the Watson-Crick to Hoogsteen exchange obtained from ^{1}H CEST and ^{13}C/^{15}N $R_{1\rho}$. (a) Comparison of exchange parameters (k_{ex} and p_{ES}) measured using ^{1}H CEST with counterparts previously reported using ^{13}C/^{15}N off-resonance $R_{1\rho}$ (Nikolova et al., 2011; Alvey et al., 2014; Shi et al., 2018). ^{13}C RD data for A18, A19 and A20 were measured using off-resonance $R_{1\rho}$ in this study (Fig. S7). Small systematic deviations in k_{ex} for the values indicated with asterisks could be due to small differences in temperature (< 0.8ºC) across different spectrometers. Bps are specified by the corresponding purine residue. (b) Comparison of the Δω obtained from fitting ^{1}H CEST profiles for T-H3 and G-H1 (Table S1) with the values expected for a Watson-Crick to Hoogsteen transition based on duplexes in which A-T or G-C$^+$ Hoogsteen bps were rendered the dominant state, by using N^1-methylated adenine (m^{1}A) (Nikolova et al., 2011; Sathyamoorthy et al., 2017; Rangadurai et al., 2020b), by binding of the drug (echinomycin) to a DNA duplex (Xu et al., 2018),

https://doi.org/10.5194/mr-2021-58
Preprint. Discussion started: 20 July 2021


Open Access MAGNETIC RESONANCE Discussions

or through use of GC repeat sequences (GC repeats) that predominantly form Hoogsteen bps at low pH (Stelling et al., 2017). (c) Comparison of free energy (ΔG°), enthalpy (ΔH°) and entropy (-TΔS°, T = 25 °C) of the Watson-Crick to Hoogsteen transition, and the activation free energy (ΔG°‡), enthalpy (ΔH°‡) and entropy (-TΔS°‡, T = 25 °C) for Watson-Crick to Hoogsteen (Watson-Crick - Hoogsteen) and Hoogsteen to Watson-Crick (Hoogsteen - Watson-Crick) transitions measured using ^{1}H CEST in this study and using ^{13}C $R_{1\rho}$ from Nikolova *et al* (Nikolova et al., 2011). The energetics in (c) were measured for the Watson-Crick to Hoogsteen transition of A16-T9 in A_6-DNA at pH 6.8. Errors in (a) were fitting errors of ^{1}H CEST, calculated as described in Methods or errors of ^{13}C/^{15}N $R_{1\rho}$ calculated using a Monte-Carlo scheme as described previously (Rangadurai et al., 2019b). Errors in (b) are the standard deviations of data points (shown as black dots) in each category. Error bars in (c) were propagated from the errors in the exchange parameters obtained from ^{1}H CEST or ^{13}C/^{15}N $R_{1\rho}$.

Indeed, the p_{ES} and k_{ex} values derived using ^{1}H CEST were in very good agreement with their off-resonance ^{13}C and/or ^{15}N $R_{1\rho}$ counterparts (Fig. 5a). The differences between k_{ex} and p_{ES} measured using the two methods was often within error with the largest differences being <3-fold. A small and systematic difference

https://doi.org/10.5194/mr-2021-58
Preprint. Discussion started: 20 July 2021


Open Access MAGNETIC RESONANCE Discussions

508 in k_{ex} was observed for a subset of the data (Fig. 5a), and this might be due to
509 small temperature differences (<0.8ºC) between spectrometers. Importantly, the
510 ES imino ^{1}H chemical shifts deduced from a 2-state fit of the ^{1}H CEST profiles
511 ($\Delta\omega_{A\text{-}T}$ = ~-1 to -2 ppm and $\Delta\omega_{G\text{-}C}$ = ~-1.5 to -2.0 ppm) were also in good agreement
512 with the expected range of values ($\Delta\omega$ = -1 to -2 ppm) for Hoogsteen bps (Fig. 5b)
513 based on studies of duplexes containing Hoogsteen bps as the dominant
514 conformation (Nikolova et al., 2011; Stelling et al., 2017; Xu et al., 2018;
515 Rangadurai et al., 2020b).
516
517 As an additional test, we also measured temperature-dependent (5 °C, 10 °C,
518 20 °C, 25 °C, 30 °C and 45 °C) ^{1}H CEST profiles for A_6-DNA at pH 6.8 (Fig. S2),
519 and then used the temperature dependence of the fitted kinetic rate constants (k_1
520 and k_{-1}) to determine the standard and activation enthalpy and entropy changes
521 for the Watson-Crick to Hoogsteen transition (Fig. S6). These values were in
522 excellent agreement with those measured from off-resonance ^{13}C $R_{1\rho}$ (Nikolova et
523 al., 2011) (Fig. 5c), further supporting the robustness of the ^{1}H CEST methodology.
524
525 **2.3 New insights into Hoogsteen breathing**

https://doi.org/10.5194/mr-2021-58
Preprint. Discussion started: 20 July 2021


Open Access MAGNETIC RESONANCE Discussions

526 ^{1}H CEST profiles for some residues show detectable exchange contributions when
527 corresponding ^{13}C/^{15}N RD measurements do not or show only weak exchange.
528 This suggests that ^{1}H CEST can provide additional insights into Watson-Crick to
529 Hoogsteen exchange and extend the detection limits of conventional ^{13}C/^{15}N RD
530 measurements.
531
532 For example, using ^{1}H CEST it was feasible to measure Watson-Crick to
533 Hoogsteen exchange for T5-H3, T6-H3, and T7-H3 (Fig. S2) within the middle of
534 the A-tract motif (defined as A_n-tract with n>3) in A_6-DNA. These residues had
535 previously exhibited only weak on-resonance ^{13}C $R_{1\rho}$ RD, and as a result, no off-
536 resonance $R_{1\rho}$ data were ever recorded (Nikolova et al., 2011). Based on the ^{1}H
537 CEST measurements, residues within the A-tract motif have ten-fold lower
538 Hoogsteen population (p_{ES} = 0.06±0.01 %-0.09±0.03 %) relative to other A-T bps
539 in A_6-DNA (p_{ES} > ~0.10 %) (Table S1). These represent the lowest A-T Hoogsteen
540 populations ever recorded to date in duplex DNA (Table S1). The exchange
541 kinetics were also 2-fold slower (k_{ex} ~1000 s^{-1}) for the A-tract residues relative to
542 other A-T bps (k_{ex} > 2000 s^{-1}) in A_6-DNA (Table S1). Interestingly, the suppression
543 of Hoogsteen dynamics within the A-tract motif appears to be A-tract length
544 dependent, with both the Hoogteen population and exchange kinetics increasing
545 slightly for similar bps in A_5-DNA (Table S1). The suppression of Hoogsteen

https://doi.org/10.5194/mr-2021-58
Preprint. Discussion started: 20 July 2021


Open Access MAGNETIC RESONANCE Discussions

546 dynamics within A-tracts is consistent with prior studies showing them to be more
547 rigid and stiff motifs relative to scrambled DNA (Nikolova et al., 2012b). We
548 verified these ^{1}H CEST derived exchange parameters for A-tract residues in A_6-
549 DNA by performing off-resonance ^{13}C $R_{1\rho}$ measurements (Fig. S7) on uniformly
550 ^{13}C/^{15}N labeled A_6-DNA and did indeed observe the expected RD with p_{ES} and k_{ex}
551 values similar (difference <3-fold, Fig. 5a) to those measured using ^{1}H CEST.
552 These prospective tests of the ^{1}H CEST data using off-resonance ^{13}C/^{15}N $R_{1\rho}$ RD
553 data further support the methodology.
554
555 The ability to characterize fast exchange kinetics has long been a motivation for
556 using ^{1}H in RD experiments to characterize conformational exchange (Ishima et
557 al., 1998; Ishima and Torchia, 2003; Eichmuller and Skrynnikov, 2005; Lundstrom
558 and Akke, 2005; Otten et al., 2010; Hansen et al., 2012; Smith et al., 2015; Steiner
559 et al., 2016; Furukawa et al., 2021). Indeed, ^{1}H CEST made it possible to measure
560 fast Watson-Crick to Hoogsteen exchange kinetics which were undetectable by
561 off-resonance ^{13}C $R_{1\rho}$. In particular, it was possible to measure Watson-Crick to
562 Hoogsteen exchange for T22 in A_6-DNA with k_{ex} > 20,000 s^{-1} (Fig. S2 and Table
563 S1), which is the fastest ever recorded Hoogsteen exchange process at 25 °C
564 (Table S1). In contrast, the off-resonance ^{13}C $R_{1\rho}$ RD profiles reported for this
565 residue in prior studies were flat (Nikolova et al., 2011; Shi et al., 2018), and

https://doi.org/10.5194/mr-2021-58
Preprint. Discussion started: 20 July 2021


Open Access MAGNETIC RESONANCE Discussions

simulations show that such an exchange process is too fast for reliable detection using ^{13}C $R_{1\rho}$ (Fig. S8a). Similarly, it was feasible to measure Watson-Crick to Hoogsteen exchange for G6 (p_{ES} ~0.3 %, k_{ex} ~3000 s^{-1}) in A_2-DNA using ^{1}H CEST yet no off-resonance ^{13}C $R_{1\rho}$ RD on C1' was previously detected (Shi et al., 2018), which based on simulations, was likely due to a combination of exchange kinetics and small Δω value (Fig. S8b).

One of the potential utilities of the ^{1}H CEST experiment is the measurement of very fast exchange kinetics at high temperatures and in a manner insensitive to melting of duplexes, shown previously to complicate analysis of Hoogsteen exchange using ^{13}C and ^{15}N RD (Shi et al., 2019). Melting of duplexes should not yield any exchange dips around the imino ^{1}H region given that the imino protons of single-stranded species (ssDNA) exchange rapidly with solvent.

We therefore measured ^{1}H CEST profiles for A_6-DNA at 45 °C (Fig. S2), in which the ssDNA population is ~10 % (Shi et al., 2019). We did not observe any evidence for the ssDNA species in the ^{1}H CEST profiles. Instead, we were able to observe ultra-fast (k_{ex} ~ 10,000 s^{-1}, see Table S1) Hoogsteen exchange which could not previously be detected by ^{13}C or ^{15}N RD experiments at the same temperature (Shi et al., 2019).

https://doi.org/10.5194/mr-2021-58
Preprint. Discussion started: 20 July 2021


Open Access MAGNETIC RESONANCE Discussions

586

587 Taken together, these results demonstrate that the ^{1}H CEST experiment broadens
588 the range of populations and exchange rates over which Hoogsteen breathing can
589 be effectively characterized.

590 ## 3 Discussion

591 Building on prior studies showing the utility of the SELOPE ^{1}H RD experiment in
592 measuring conformational exchange in unlabeled RNA (Schlagnitweit et al., 2018)
593 and DNA (Furukawa et al., 2021; Dubini et al., 2020), our study establishes the
594 utility of high-power ^{1}H CEST SELOPE as a facile means for measuring the
595 Watson-Crick to Hoogsteen exchange process in nucleic acids without the need
596 for isotopic enrichment. The methodology is supported by the very good
597 agreement observed between the measured exchange parameters and values
598 measured independently using ^{13}C and/or ^{15}N $R_{1\rho}$ for a variety of bps in three
599 duplexes under different conditions of temperature and pH, as well as by the good
600 agreement seen between the imino ^{1}H chemical shifts and those expected based
601 on duplexes containing Hoogsteen bps as the dominant GS conformation. The
602 high throughput nature of the experiment and simple sample requirements enabled
603 us to measure Hoogsteen dynamics for 37 data points corresponding to 22 distinct

https://doi.org/10.5194/mr-2021-58
Preprint. Discussion started: 20 July 2021


Open Access MAGNETIC RESONANCE Discussions

604 bps for three different pH conditions and seven different temperatures (Table S1),
605 the largest collection of Hoogsteen dynamics from a single study to date. We
606 envision using the ^{1}H CEST SELOPE experiments to pre-screen DNA duplexes
607 and to perform follow-up ^{13}C and ^{15}N RD experiments to confirm any interesting
608 outliers, particularly regions showing substantially elevated Hoogsteen dynamics.
609
610 An important consideration when applying ^{1}H CEST to the study of chemical
611 exchange are contributions due to ^{1}H-^{1}H cross-relaxation originating from cross
612 relaxation, which may give rise to extraneous NOE dips that complicate data
613 analysis (Yuwen et al., 2017a; Bouvignies and Kay, 2012; Eichmuller and
614 Skrynnikov, 2005). These contributions have been shown to be significant in
615 proteins particularly when characterizing slow exchange (k_{ex} < 200 s^{-1})
616 necessitating use of relatively long relaxation delays (Bouvignies and Kay, 2012).
617 Consistent with prior studies of nucleic acids (Schlagnitweit et al., 2018; Steiner et
618 al., 2016; Baronti et al., 2020) and proteins (Lundstrom and Akke, 2005), our
619 results indicate that NOE effects involving imino protons can be effectively
620 suppressed for DNA and RNA duplexes in the ^{1}H CEST experiments through
621 selective excitation provided that the relaxation delays are short on the order of
622 100 ms (Fig. 3b). However, because NOE dips were clearly visible when using
623 400 ms relaxation delay, care should be exercised on a case-by-case basis to

https://doi.org/10.5194/mr-2021-58
Preprint. Discussion started: 20 July 2021


Open Access MAGNETIC RESONANCE Discussions

624 evaluate NOE effects (Fig. 3b), which may also be more substantial for certain
625 non-canonical motifs. In addition to cross-referencing the dip with 2D [^{1}H, ^{1}H]
626 NOESY spectra, testing whether the dip increases in magnitude without selective
627 excitation can help to distinguish between dips due to an ES versus NOE effects.
628
629 Prior studies showed that Watson-Crick to Hoogsteen bp transitions exhibit large
630 variations in the forward rate constants (k_1) while the backward rate constants (k_{-1})
631 is relatively constant across different sequence contexts, consistent with a late
632 transitional state (Alvey et al., 2014). We observe a similar trend in which k_{-1} varied
633 <5-fold while k_1 varied by ~50-fold (Fig. S9). The ^{1}H CEST data also revealed
634 significantly lower Hoogsteen abundance (p_{ES} < 0.1 %) in addition to slower
635 exchange kinetics (k_{ex} ~1,000 s^{-1}) within A-tract motifs (Nikolova et al., 2011; Alvey
636 et al., 2014), while also reinforcing prior data (Xu et al., 2018) suggesting increased
637 exchange kinetics near terminal ends. Collectively, these data show that the
638 Hoogsteen population can vary by as much as ~14-fold while k_{ex} can vary by ~20-
639 fold only due to changes in sequence and positional context (Table S1). These
640 strong sequence and position dependencies could play important roles in
641 biochemical processes acting on DNA.
642

https://doi.org/10.5194/mr-2021-58
Preprint. Discussion started: 20 July 2021


Open Access MAGNETIC RESONANCE Discussions

643 A recent study (Furukawa et al., 2021) reported on-resonance imino ^{1}H $R_{1\rho}$ RD for
644 a guanine residue in a DNA duplex at pH = 7.5, T= 30 °C, and in 150 mM NaCl.
645 Because off-resonance measurements were not performed, only k_{ex} ~ 10,000 s^{-1}
646 could be determined while the values of Δω and p_{ES} were not determined. The
647 study noted that a Hoogsteen bp as the ES was unlikely given that G-C^{+} Hoogsteen
648 bps are disfavored at pH= 7.5 and because the observed rate of exchange (k_{ex} ~
649 10,000 s^{-1}) was much faster than is typically observed for Watson-Crick to
650 Hoogsteen exchange. Instead, the data were interpreted as evidence for a base
651 opened state. However, the observed rate of exchange k_{ex} ~10,000 s^{-1} falls
652 comfortably within the range of values measured here for Watson-Crick to
653 Hoogsteen exchange using ^{1}H CEST at similar pH conditions. For example, for
654 the G10-C15 bp in A_6-DNA at the same temperature and pH = 6.8, k_{ex} for Watson-
655 Crick to Hoogsteen exchange was ~6,000 s^{-1} (Fig. 4 and Table S1). Similar
656 Watson-Crick to Hoogsteen exchange parameters (p_{ES} ~0.05 % and k_{ex} ~2000 s^{-1}
657) were recently reported for this bp at 25 °C and pH 6.8 using cytosine amino ^{15}N
658 RD (Rangadurai et al., 2019a) and the ES $\Delta\omega_{C\text{-}N4}$ = -9 ppm was shown to be in
659 excellent agreement with values expected for a G-C^{+} Hoogsteen bp. In addition,
660 based on hydrogen exchange measurements, p_{ES} ~0.00001 % to 0.01 % and k_{ex}
661 (k_{cl} + k_{op}, k_{cl} and k_{op} are the base closing and opening rate constant, respectively)
662 ~ 10^{5} to 10^{7} s^{-1} for the base-opened ES, and this process should fall outside RD

https://doi.org/10.5194/mr-2021-58
Preprint. Discussion started: 20 July 2021


Open Access MAGNETIC RESONANCE Discussions

detection (Gueron and Leroy, 1995; Gueron et al., 1987; Leroy et al., 1988; Leijon and Graslund, 1992; Snoussi and Leroy, 2001). Therefore, the ES detected by Furukawa *et al* (Furukawa et al., 2021) is more likely a Hoogsteen bp.

In conclusion, by obviating the need for isotopic enrichment, the ^{1}H CEST experiment expands the scope of characterizing Watson-Crick to Hoogsteen exchange in nucleic acids by NMR. We are presently applying the experiment to map the sequence dependence of Hoogsteen breathing dynamics and systematically, how it varies with pH, salt, and crowding, and following the introduction of lesions, mismatches, and molecules that bind to the DNA.

https://doi.org/10.5194/mr-2021-58
Preprint. Discussion started: 20 July 2021


Open Access MAGNETIC RESONANCE Discussions

673 # 4 Methods

674 ## 4.1 Sample preparation

675 *Unlabeled DNA and RNA oligonucleotides*: Unmodified DNA oligonucleotides
676 were purchased from Integrated DNA Technologies with standard desalting
677 purification. RNA oligonucleotides were synthesized using a MerMade 6 Oligo
678 Synthesizer employing 2'-tBDSilyl protected phosphoramidites (n-acetyl protected
679 rC, rA and rG, and rU phosphoramidites were purchased from Chemgenes) and 1
680 µmol standard synthesis columns (1000 Å) (BioAutomation). RNA
681 oligonucleotides were synthesized with the final 5'-protecting group, 4,4'-
682 dimethoxytrityl (DMT) retained. RNA oligonucleotides were cleaved from columns
683 using 1 ml AMA (1:1 ratio of 30 % ammonium hydroxide and 30 % methylamine)
684 and incubated at room temperature for 2 hours. The sample was then air-dried
685 and dissolved in 115 µL DMSO, 60 µL TEA, and 75uL TEA.3HF, and then
686 incubated at T = 65 °C for 2.5 hours to remove 2'-O protecting groups. The Glen-
687 Pak RNA cartridges (Glen Research Corporation) were then used to purify the
688 samples followed by ethanol precipitation.

689

690 *Labeled DNA oligonucleotides*: The uniformly ^{13}C, ^{15}N labeled A_6-DNA sample was
691 prepared using chemically synthesized DNA (purchased from IDT), Klenow

https://doi.org/10.5194/mr-2021-58
Preprint. Discussion started: 20 July 2021


Open Access MAGNETIC RESONANCE Discussions

692 fragment DNA polymerase (New England Biolab) and $^{13}C/^{15}N$ isotopically labeled
693 dNTPs (Silantes) using the Zimmer and Crothers method (Zimmer and Crothers,
694 1995). The oligonucleotide was purified using 20 % 29:1 polyacrylamide
695 denaturing gel with 8 M urea, 20 mM Tris borate and 1 mM EDTA, and then using
696 electro-elution (Whatmann, GE Healthcare) in 40 mM Tris Acetate and 1 mM
697 EDTA, followed by ethanol precipitation.
698
699 *Sample annealing and buffer exchange*: DNA/RNA oligonucleotides were re-
700 suspended in water (200-500 µM). To prepare duplex samples, equimolar
701 amounts of the constituent single stranded DNA/RNA samples were mixed and
702 then heated at T = 95 °C for ~5 min followed by cooling at room temperature for
703 ~1 hour. All samples were exchanged three times into the desired buffer using
704 centrifugal concentrators (4 mL, Millipore Sigma). 10 % D_2O (Millipore Sigma) was
705 added to the samples prior to the NMR measurements.
706
707 *Sample concentrations and buffer conditions*: Unless mentioned otherwise, the
708 NMR buffer contains 25 mM sodium chloride, 15 mM sodium phosphate, 0.1 mM
709 EDTA and 10 % D_2O. Sample concentrations and buffer pH: A_6-DNA, 1.0 mM, pH
710 6.8; A_2-DNA, 1.0 mM, pH 5.4; A_5-DNA, 0.2 mM, pH 5.2; A_6-RNA, 0.5 mM, pH 6.8.
711 Concentration was estimated by measuring the absorbance of the sample at

https://doi.org/10.5194/mr-2021-58
Preprint. Discussion started: 20 July 2021


Open Access MAGNETIC RESONANCE Discussions

260nm and using extinction coefficients from the ADT Biol Oligo calculator (https://www.atdbio.com/tools/oligo-calculator).

4.2 NMR spectroscopy

All NMR experiments were performed on a 600 BrukerAvance 3 spectrometer equipped with a triple-resonance HCN cryo-genic probe. The NMR data were processed and analyzed with NMRpipe (Delaglio et al., 1995) and SPARKY (T.D. Goddard and D.G. Kneller, SPARKY 3, University of California, San Francisco).

Resonance assignments: Imino resonances were assigned using a combination of 2D [^{1}H, ^{1}H] NOESY and [^{15}N,^{1}H] SOFAST-HMQC (Sathyamoorthy et al., 2014) experiments. Assignments for A_6-DNA, A_2-DNA and A_6-RNA were reported previously (Sathyamoorthy et al., 2017; Zhou et al., 2016; Nikolova et al., 2011). The [^{1}H, ^{1}H] NOESY spectrum for A_5-DNA is shown in Fig. S1.

^{1}H CEST: The pulse sequence was shown in Fig. 1b, and was adapted from Schlagnitweit *et al* (Schlagnitweit et al., 2018). Relaxation delays T_{EX} = 100 ms was used for all ^{1}H CEST measurements at low temperatures (5 °C – 30 °C), while a shorter T_{EX} = 80 ms was used for high (45 °C) temperature measurements. A

https://doi.org/10.5194/mr-2021-58
Preprint. Discussion started: 20 July 2021


Open Access MAGNETIC RESONANCE Discussions

longer T_{EX} = 400 ms was used to illustrate artefacts arising due to NOE dips (Fig. 3b). RF power and offset combinations used in the CEST measurements are given in Table S2. Calibration of RF field powers for the ^{1}H CEST measurements was performed as described previously (Rangadurai et al., 2019b) using the same pulse sequence. Field inhomogeneity was also measured (Fig. S10) using the same sequence and the procedure as described previously (Guenneugues et al., 1999). ^{1}H inhomogeneity was measured by performing on-resonance ^{1}H CEST experiments on G2-H1 of A_6-DNA, chosen as it does not experience conformational exchange. The longest relaxation delay used for the measurements were 10 s, 2 s, 1 s, 0.4 s, 0.1 s and 0.04 s for RF fields 10 Hz, 50 Hz, 100 Hz, 200 Hz, 1000 Hz and 4000 Hz, respectively. The resulting nutation curve was Fourier transformed and was fit to a gaussian function (blue lines in Fig. S10) to extract the full-width at half-maximum, which was used for defining the inhomogeneity as described previously (Guenneugues et al., 1999). The selective pulse was set to be off (Fig. 3b) by replacing pulse **a** (Fig. 1b) with a non-selective ^{1}H hard 90° pulse.

Fitting of ^{1}H CEST data: When performing 2-state CEST fitting with and without exchange, we restricted the offset to -6 to 6 ppm for ^{1}H CEST experiment with relaxation delay ≤ 100 ms, and to -3 to 3 ppm for experiments with relaxation delay

https://doi.org/10.5194/mr-2021-58
Preprint. Discussion started: 20 July 2021


Open Access MAGNETIC RESONANCE Discussions

751 = 400 ms, to obviate any potential effects from ^{1}H-^{1}H cross-relaxation artifacts (Fig.
752 3b). Peak intensities of all imino protons in the 1D spectra as a function of RF
753 power and offset frequency were extracted using NMRPipe (Delaglio et al., 1995).
754 The peak intensity at a given RF power and offset is normalized by the average
755 peak intensity over the triplicate CEST measurements with zero relaxation delay
756 under the same RF power. The uncertainty in the measured peak intensity at each
757 offset frequency and RF power combination was assumed to be equal to the
758 standard deviation of the peak intensities for triplicate CEST experiments with zero
759 relaxation delay under the same RF power (Zhao et al., 2014; Shi et al., 2019).
760 CEST profiles were generated by plotting the normalized intensity as a function of
761 offset $\Omega = \omega_{RF} - \omega_{obs}$ where ω_{obs} is the Larmor frequency of the observed
762 resonance and ω_{RF} is the angular frequency of the applied RF field. RF field
763 inhomogeneity (Fig. S10) was taken into account during CEST fitting as described
764 previously (Rangadurai et al., 2020a). The normalized CEST profiles were then fit
765 via numerical integration of the Bloch-McConnell (B-M) equations as described
766 previously (Rangadurai et al., 2020a). Fitting of CEST profiles without exchange
767 (Fig. 4, Fig. S2-4) was performed by setting $p_{ES} = k_{ex} = \Delta\omega = 0$. Errors in exchange
768 parameters were set to be equal to the fitting errors which were obtained as the
769 square root of the diagonal elements of the covariance matrix. Reduced chi-

https://doi.org/10.5194/mr-2021-58
Preprint. Discussion started: 20 July 2021


Open Access MAGNETIC RESONANCE Discussions

770 square ($r\chi^2$) was calculated to assess the goodness of fitting (Rangadurai et al.,
771 2019b). The residual sum of squares (RSS) was computed as follows

772 $$RSS = \sum_{i=1}^{n} \left(I_i^{fit} - I_i^{exp}\right)^2 \quad (1)$$

773 *where* I_i^{fit} and I_i^{exp} are the *i*th fit and experimentally measured intensity in the
774 CEST profile respectively, and the summation is over all RF power and offset
775 combinations (N).

776

777 Model selection for fits with and without exchange (Fig. 4, Fig. S2-4) was
778 performed by computing AIC and BIC weights as follows (Burnham and Anderson,
779 2004):

780

781 $$AIC = \begin{cases} Nln\left(\frac{RSS}{N}\right) + 2K, & when \frac{N}{K} \geq 40 \\ Nln\left(\frac{RSS}{N}\right) + 2K + \frac{2K(K+1)}{N-K-1}, & when \frac{N}{K} < 40 \end{cases} \quad (2)$$

782

783 $$wAIC = \frac{e^{-0.5\Delta AIC}}{1 + e^{-0.5\Delta AIC}} \quad (3)$$

784

785 $$BIC = Nln\left(\frac{RSS}{N}\right) + Kln(N) \quad (4)$$

786

787 $$wBIC = \frac{e^{-0.5\Delta BIC}}{1 + e^{-0.5\Delta BIC}} \quad (5)$$

https://doi.org/10.5194/mr-2021-58
Preprint. Discussion started: 20 July 2021


Open Access MAGNETIC RESONANCE Discussions

788

789 Where *K* is the number of floating parameters when fitting and $\Delta AIC/\Delta BIC$ are the
790 differences between two AIC values (fitting without and with exchange). The AIC
791 ($wAIC_{+ex}$) and BIC ($wBIC_{+ex}$) weights for fits with exchange are reported in Fig. 4
792 and Fig. S2-4. The improvement in the fit was considered statistically significant if
793 both $wAIC_{+ex}$ and $wBIC_{+ex}$ values are > 0.995, and $r\chi^2$ is reduced with the inclusion
794 of exchange. For some resonances, the improvement in the fit with exchange are
795 statistically significant but the resulting exchange parameters are not reliable and
796 have large errors (see Fig. S2,3). For T4 in A_5-DNA, p_{ES} = 0.2±0.1 % measured
797 using ^{1}H CEST was ~10-fold smaller than p_{ES} = 2.7±1.5 % measured previously
798 using ^{15}N RD (Alvey et al., 2014), whereas k_{ex} (~3000 s^{-1}) was is in good
799 agreement. However, simulations show that due to the small Δω for ^{15}N (~1 ppm)
800 and fast exchange kinetics k_{ex} (~3000 s^{-1}) the p_{ES} and Δω are not well-determined
801 by the ^{15}N RD data (Fig. S6c). For this reason, this data point was excluded for ^{1}H
802 CEST and ^{13}C/^{15}N RD comparison (Fig. 5a).

803

804 *Off-resonance ^{13}C $R_{1\rho}$ relaxation dispersion*: ^{13}C $R_{1\rho}$ experiments were performed
805 using 1D $R_{1\rho}$ schemes as described previously (Nikolova et al., 2012a; Nikolova
806 et al., 2011; Hansen et al., 2009). The spin-lock powers and offsets are listed in
807 Table S3. The spin-lock was applied for a maximal duration < 60 ms to achieve

https://doi.org/10.5194/mr-2021-58
Preprint. Discussion started: 20 July 2021


Open Access MAGNETIC RESONANCE Discussions

~70 % loss of peak intensity at the end of relaxation delay. Off-resonance $R_{1\rho}$ profiles (Fig. S8) were generated by plotting (R_2 + R_{ex}) = ($R_{1\rho}$ - $R_1\cos^2\theta$)/$\sin^2\theta$, where θ is the angle between the effective field of the observed resonance and the z-axis, as a function of $\Omega_{eff}/2\pi$, where $\Omega_{eff} = \omega_{obs} - \omega_{RF}$, where ω_{obs} is the Larmor frequency of the spin and ω_{RF} is the carrier frequency of the applied spin-lock.

Fitting of ^{13}C $R_{1\rho}$ data: 1D peak intensities were measured using NMRpipe (Delaglio et al., 1995). $R_{1\rho}$ values for a given spin-lock power and offset were calculated by fitting the intensities as a function of delay time to a mono-exponential decay (Kimsey et al., 2015). A Monte-Carlo approach was used to calculate the uncertainties of $R_{1\rho}$ (Bothe et al., 2014). Alignment of initial magnetization during the Bloch-McConnell fitting was performed based on the $k_{ex}/\Delta\omega$ value (Rangadurai et al., 2019b). Chemical exchange parameters were obtained by fitting experimental $R_{1\rho}$ values to numerical solutions of a 2-state Bloch-McConnell (B-M) equations (Mcconnell, 1958). A Monte-Carlo approach was used to calculate the errors of exchange parameters (Bothe et al., 2014) . Reduced chi-square ($r\chi^2$) was calculated to assess the goodness of fitting (Rangadurai et al., 2019b).

4.3 Thermodynamic Analysis

https://doi.org/10.5194/mr-2021-58
Preprint. Discussion started: 20 July 2021


Open Access MAGNETIC RESONANCE Discussions

The observed temperature dependence of k_1, k_{-1} for the Watson-Crick to Hoogsteen exchange measuring using ^{1}H CEST were fit to a modified van't Hoff equation that accounts for statistical compensation effects and assumes a smooth energy surface as described previously (Nikolova et al., 2011; Coman and Russu, 2005):

$$\ln\left(\frac{k_i(T)}{T}\right) = \ln\left(\frac{k_B\kappa}{h}\right) - \frac{\Delta G_i^{\circ T}(T_{hm})}{RT_{hm}} - \frac{\Delta H_i^{\circ T}}{R}\left(\frac{1}{T} - \frac{1}{T_{hm}}\right) \quad (6)$$

k_i (i = 1, -1) is the forward and backward rate constants, $\Delta G_i^{\circ T}(T)$ and $\Delta H_i^{\circ T}$ are the free energy (at temperature T, in Kelvin) and enthalpy of activation (i = 1) or deactivation (i = -1) respectively. R is the universal gas constant (kcal mol^{-1} K^{-1}) and T_{hm} is the harmonic mean of the experimental temperatures (T_i in K) computed as $T_{hm} = n/\sum_{i=1}^{n}(1/T_i)$, k_B is the Boltzmann's constant (J K^{-1}), κ is the transmission coefficient (assumed to be unity) and h is the Planck constant (J s).

The goodness-of-fit indicator R^2 (coefficient of determination) (Fig. S6) between the measured and fitted rate constants was calculated as follows: $R^2 = 1 - \frac{SS_{res}}{SS_{total}}, SS_{res} = \sum(k_{i,fit} - k_{i,exp})^2$, $SS_{total} = \sum(k_{i,exp} - \overline{k_{i,exp}})^2$. $k_{i,fit}$ and $k_{i,exp}$ (i = 1, -1) are fitted and experimentally measured rate constants. $\overline{k_{i,exp}}$ is the mean

https://doi.org/10.5194/mr-2021-58
Preprint. Discussion started: 20 July 2021

Open Access MAGNETIC RESONANCE Discussions

of all $k_{i,exp}$. Errors of fitting for $\Delta G_i^{\circ T}$ and ΔH_i^T were calculated as the square root of the diagonal elements of the covariance matrix. $T\Delta S_i^T$ is calculated as $\Delta H_i^T - \Delta G_i^{\circ T}$.

https://doi.org/10.5194/mr-2021-58
Preprint. Discussion started: 20 July 2021


Open Access MAGNETIC RESONANCE Discussions

850 **Data and code availability.** The data that support this study are contained in the
851 published article (and its Supplementary Information) or are available from the
852 corresponding author on reasonable request. The python scripts for ^{1}H CEST data
853 fitting are available at https://github.com/alhashimilab/1H-CEST.

854

855 **Author contributions.** BL, AR, and HMA conceived the project and experimental
856 design. BL, AR, and HS prepared the samples and set up the imino ^{1}H CEST
857 experiment. BL performed ^{1}H CEST experiments and data analysis. HS
858 performed ^{13}C $R_{1\rho}$ experiments. HMA, BL, and AR wrote the manuscript with
859 critical input from HS.

860

861 **Competing interests.** The authors declare that they have no conflict of interest.

862

863 **Acknowledgments.** We thank Prof. Katja Petzold for sharing the ^{1}H CEST pulse
864 sequence. We thank Dr. Or Szekely for general input and Ainan Geng for help
865 with the ^{1}H inhomogeneity measurements.

866

867 **Financial Support.** This work was supported by the US National Institutes of
868 Health (R01GM089846) Grants to H.M.A.

https://doi.org/10.5194/mr-2021-58
Preprint. Discussion started: 20 July 2021

Open Access MAGNETIC RESONANCE Discussions

Reference

Afek, A., Shi, H., Rangadurai, A., Sahay, H., Senitzki, A., Xhani, S., Fang, M., Salinas, R., Mielko, Z., Pufall, M. A., Poon, G. M. K., Haran, T. E., Schumacher, M. A., Al-Hashimi, H. M., and Gordan, R.: DNA mismatches reveal conformational penalties in protein-DNA recognition, Nature, 587, 291-296, 10.1038/s41586-020-2843-2, 2020.

Aishima, J., Gitti, R. K., Noah, J. E., Gan, H. H., Schlick, T., and Wolberger, C.: A Hoogsteen base pair embedded in undistorted B-DNA, Nucleic acids research, 30, 5244-5252, 2002.

Alvey, H. S., Gottardo, F. L., Nikolova, E. N., and Al-Hashimi, H. M.: Widespread transient Hoogsteen base pairs in canonical duplex DNA with variable energetics, Nat Commun, 5, 4786, 10.1038/ncomms5786, 2014.

Baronti, L., Guzzetti, I., Ebrahimi, P., Friebe Sandoz, S., Steiner, E., Schlagnitweit, J., Fromm, B., Silva, L., Fontana, C., Chen, A. A., and Petzold, K.: Base-pair conformational switch modulates miR-34a targeting of Sirt1 mRNA, Nature, 583, 139-144, 10.1038/s41586-020-2336-3, 2020.

Ben Imeddourene, A., Zargarian, L., Buckle, M., Hartmann, B., and Mauffret, O.: Slow motions in A.T rich DNA sequence, Sci Rep, 10, 19005, 10.1038/s41598-020-75645-x, 2020.

Bothe, J. R., Stein, Z. W., and Al-Hashimi, H. M.: Evaluating the uncertainty in exchange parameters determined from off-resonance R1rho relaxation dispersion for systems in fast exchange, J Magn Reson, 244, 18-29, 10.1016/j.jmr.2014.04.010, 2014.

Bouvignies, G. and Kay, L. E.: Measurement of proton chemical shifts in invisible states of slowly exchanging protein systems by chemical exchange saturation transfer, J Phys Chem B, 116, 14311-14317, 10.1021/jp311109u, 2012.

Burnham, K. P. and Anderson, D. R.: Multimodel inference - understanding AIC and BIC in model selection, Sociol Method Res, 33, 261-304, 10.1177/0049124104268644, 2004.

Chen, B., LeBlanc, R., and Dayie, T. K.: SAM-II Riboswitch Samples at least Two Conformations in Solution in the Absence of Ligand: Implications for Recognition, Angew Chem Int Edit, 55, 2724-2727, 10.1002/anie.201509997, 2016.

Coman, D. and Russu, I. M.: A nuclear magnetic resonance investigation of the energetics of basepair opening pathways in DNA, Biophys J, 89, 3285-3292, 10.1529/biophysj.105.065763, 2005.

Czernek, J., Fiala, R., and Sklenar, V.: Hydrogen bonding effects on the (15)N and (1)H shielding tensors in nucleic acid base pairs, J Magn Reson, 145, 142-146, 10.1006/jmre.2000.2091, 2000.

Delaglio, F., Grzesiek, S., Vuister, G. W., Zhu, G., Pfeifer, J., and Bax, A.: NMRPipe: a multidimensional spectral processing system based on UNIX pipes, J Biomol NMR, 6, 277-293, 10.1007/BF00197809, 1995.

Dubini, R. C. A., Schon, A., Muller, M., Carell, T., and Rovo, P.: Impact of 5-formylcytosine on the melting kinetics of DNA by 1H NMR chemical exchange, Nucleic Acids Res, 48, 8796-8807, 10.1093/nar/gkaa589, 2020.

Eichmuller, C. and Skrynnikov, N. R.: A new amide proton R1rho experiment permits accurate characterization of microsecond time-scale conformational exchange, J Biomol NMR, 32, 281-293,

https://doi.org/10.5194/mr-2021-58
Preprint. Discussion started: 20 July 2021


Open Access MAGNETIC RESONANCE Discussions

10.1007/s10858-005-0658-y, 2005.
Felsenfeld, G., Davies, D. R., and Rich, A.: Formation of a 3-Stranded Polynucleotide Molecule, Journal of the American Chemical Society, 79, 2023-2024, DOI 10.1021/ja01565a074, 1957.
Frank, A. T., Horowitz, S., Andricioaei, I., and Al-Hashimi, H. M.: Utility of 1H NMR chemical shifts in determining RNA structure and dynamics, J Phys Chem B, 117, 2045-2052, 10.1021/jp310863c, 2013.
Furukawa, A., Walinda, E., Arita, K., and Sugase, K.: Structural dynamics of double-stranded DNA with epigenome modification, Nucleic Acids Res, 49, 1152-1162, 10.1093/nar/gkaa1210, 2021.
Golovenko, D., Brauning, B., Vyas, P., Haran, T. E., Rozenberg, H., and Shakked, Z.: New Insights into the Role of DNA Shape on Its Recognition by p53 Proteins, Structure, 26, 1237-1250 e1236, 10.1016/j.str.2018.06.006, 2018.
Guenneugues, M., Berthault, P., and Desvaux, H.: A method for determining B1 field inhomogeneity. Are the biases assumed in heteronuclear relaxation experiments usually underestimated?, J Magn Reson, 136, 118-126, 10.1006/jmre.1998.1590, 1999.
Gueron, M. and Leroy, J. L.: Studies of base pair kinetics by NMR measurement of proton exchange, Methods Enzymol, 261, 383-413, 10.1016/s0076-6879(95)61018-9, 1995.
Gueron, M., Kochoyan, M., and Leroy, J. L.: A single mode of DNA base-pair opening drives imino proton exchange, Nature, 328, 89-92, 10.1038/328089a0, 1987.
Hansen, A. L., Lundstrom, P., Velyvis, A., and Kay, L. E.: Quantifying millisecond exchange dynamics in proteins by CPMG relaxation dispersion NMR using side-chain 1H probes, J Am Chem Soc, 134, 3178-3189, 10.1021/ja210711v, 2012.
Hansen, A. L., Nikolova, E. N., Casiano-Negroni, A., and Al-Hashimi, H. M.: Extending the range of microsecond-to-millisecond chemical exchange detected in labeled and unlabeled nucleic acids by selective carbon R(1rho) NMR spectroscopy, J Am Chem Soc, 131, 3818-3819, 10.1021/ja8091399, 2009.
Hoogsteen, K.: The Structure of Crystals Containing a Hydrogen-Bonded Complex of 1-Methylthymine and 9-Methyladenine, Acta Crystallogr, 12, 822-823, Doi 10.1107/S0365110x59002389, 1959.
Hwang, T. L. and Shaka, A. J.: Water Suppression That Works - Excitation Sculpting Using Arbitrary Wave-Forms and Pulsed-Field Gradients, J Magn Reson Ser A, 112, 275-279, DOI 10.1006/jmra.1995.1047, 1995.
Ishima, R. and Torchia, D. A.: Extending the range of amide proton relaxation dispersion experiments in proteins using a constant-time relaxation-compensated CPMG approach, J Biomol NMR, 25, 243-248, 10.1023/a:1022851228405, 2003.
Ishima, R., Wingfield, P. T., Stahl, S. J., Kaufman, J. D., and Torchia, D. A.: Using amide H-1 and N-15 transverse relaxation to detect millisecond time-scale motions in perdeuterated proteins: Application to HIV-1 protease, Journal of the American Chemical Society, 120, 10534-10542, DOI 10.1021/ja981546c, 1998.
Juen, M. A., Wunderlich, C. H., Nussbaumer, F., Tollinger, M., Kontaxis, G., Konrat, R., Hansen, D.

https://doi.org/10.5194/mr-2021-58
Preprint. Discussion started: 20 July 2021

Open Access MAGNETIC RESONANCE Discussions

947 F., and Kreutz, C.: Excited States of Nucleic Acids Probed by Proton Relaxation Dispersion NMR
948 Spectroscopy, Angew Chem Int Ed Engl, 55, 12008-12012, 10.1002/anie.201605870, 2016.
949 Kimsey, I. J., Petzold, K., Sathyamoorthy, B., Stein, Z. W., and Al-Hashimi, H. M.: Visualizing
950 transient Watson-Crick-like mispairs in DNA and RNA duplexes, Nature, 519, 315-320,
951 10.1038/nature14227, 2015.
952 Kimsey, I. J., Szymanski, E. S., Zahurancik, W. J., Shakya, A., Xue, Y., Chu, C. C., Sathyamoorthy,
953 B., Suo, Z., and Al-Hashimi, H. M.: Dynamic basis for dG*dT misincorporation via tautomerization
954 and ionization, Nature, 554, 195-201, 10.1038/nature25487, 2018.
955 Kitayner, M., Rozenberg, H., Rohs, R., Suad, O., Rabinovich, D., Honig, B., and Shakked, Z.:
956 Diversity in DNA recognition by p53 revealed by crystal structures with Hoogsteen base pairs, Nat
957 Struct Mol Biol, 17, 423-429, 10.1038/nsmb.1800, 2010.
958 Lam, S. L. and Chi, L. M.: Use of chemical shifts for structural studies of nucleic acids, Prog Nucl
959 Magn Reson Spectrosc, 56, 289-310, 10.1016/j.pnmrs.2010.01.002, 2010.
960 Lane, A. N., Bauer, C. J., and Frenkiel, T. A.: Determination of conformational transition rates in the
961 trp promoter by 1H NMR rotating-frame T1 and cross-relaxation rate measurements, Eur Biophys
962 J, 21, 425-431, 10.1007/BF00185870, 1993.
963 LeBlanc, R. M., Longhini, A. P., Tugarinov, V., and Dayie, T. K.: NMR probing of invisible excited
964 states using selectively labeled RNAs, J Biomol NMR, 71, 165-172, 10.1007/s10858-018-0184-3,
965 2018.
966 Leijon, M. and Graslund, A.: Effects of sequence and length on imino proton exchange and base
967 pair opening kinetics in DNA oligonucleotide duplexes, Nucleic Acids Res, 20, 5339-5343,
968 10.1093/nar/20.20.5339, 1992.
969 Leroy, J. L., Kochoyan, M., Huynh-Dinh, T., and Gueron, M.: Characterization of base-pair opening
970 in deoxynucleotide duplexes using catalyzed exchange of the imino proton, J Mol Biol, 200, 223-
971 238, 10.1016/0022-2836(88)90236-7, 1988.
972 Ling, H., Boudsocq, F., Plosky, B. S., Woodgate, R., and Yang, W.: Replication of a cis-syn thymine
973 dimer at atomic resolution, Nature, 424, 1083-1087, 10.1038/nature01919, 2003.
974 Liu, B., Shi, H., Rangadurai, A., Nussbaumer, F., Chu, C. C., Erharter, K., Case, D. A., Kreutz, C.,
975 and Al-Hashimi, H. M.: A quantitative model predicts how m6A reshapes the kinetic landscape of
976 nucleic acid hybridization and conformational transitions, bioRxiv, 2020.
977 Lu, L., Yi, C., Jian, X., Zheng, G., and He, C.: Structure determination of DNA methylation lesions
978 N1-meA and N3-meC in duplex DNA using a cross-linked protein-DNA system, Nucleic Acids Res,
979 38, 4415-4425, 10.1093/nar/gkq129, 2010.
980 Lundstrom, P. and Akke, M.: Off-resonance rotating-frame amide proton spin relaxation
981 experiments measuring microsecond chemical exchange in proteins, J Biomol NMR, 32, 163-173,
982 10.1007/s10858-005-5027-3, 2005.
983 Lundstrom, P., Hansen, D. F., Vallurupalli, P., and Kay, L. E.: Accurate measurement of alpha proton
984 chemical shifts of excited protein states by relaxation dispersion NMR spectroscopy, Journal of the
985 American Chemical Society, 131, 1915-1926, 10.1021/ja807796a, 2009.

https://doi.org/10.5194/mr-2021-58
Preprint. Discussion started: 20 July 2021


Open Access MAGNETIC RESONANCE Discussions

Mcconnell, H. M.: Reaction Rates by Nuclear Magnetic Resonance, J Chem Phys, 28, 430-431, Doi 10.1063/1.1744152, 1958.

Nair, D. T., Johnson, R. E., Prakash, L., Prakash, S., and Aggarwal, A. K.: Hoogsteen base pair formation promotes synthesis opposite the 1,N6-ethenodeoxyadenosine lesion by human DNA polymerase iota, Nat Struct Mol Biol, 13, 619-625, 10.1038/nsmb1118, 2006.

Nikolova, E. N., Gottardo, F. L., and Al-Hashimi, H. M.: Probing transient Hoogsteen hydrogen bonds in canonical duplex DNA using NMR relaxation dispersion and single-atom substitution, J Am Chem Soc, 134, 3667-3670, 10.1021/ja2117816, 2012a.

Nikolova, E. N., Bascom, G. D., Andricioaei, I., and Al-Hashimi, H. M.: Probing Sequence-Specific DNA Flexibility in A-Tracts and Pyrimidine-Purine Steps by Nuclear Magnetic Resonance C-13 Relaxation and Molecular Dynamics Simulations, Biochemistry, 51, 8654-8664, 10.1021/bi3009517, 2012b.

Nikolova, E. N., Goh, G. B., Brooks, C. L., 3rd, and Al-Hashimi, H. M.: Characterizing the protonation state of cytosine in transient G.C Hoogsteen base pairs in duplex DNA, J Am Chem Soc, 135, 6766-6769, 10.1021/ja400994e, 2013a.

Nikolova, E. N., Kim, E., Wise, A. A., O'Brien, P. J., Andricioaei, I., and Al-Hashimi, H. M.: Transient Hoogsteen base pairs in canonical duplex DNA, Nature, 470, 498-502, 10.1038/nature09775, 2011.

Nikolova, E. N., Zhou, H., Gottardo, F. L., Alvey, H. S., Kimsey, I. J., and Al-Hashimi, H. M.: A historical account of Hoogsteen base-pairs in duplex DNA, Biopolymers, 99, 955-968, 10.1002/bip.22334, 2013b.

Otten, R., Villali, J., Kern, D., and Mulder, F. A.: Probing microsecond time scale dynamics in proteins by methyl (1)H Carr-Purcell-Meiboom-Gill relaxation dispersion NMR measurements. Application to activation of the signaling protein NtrC(r), J Am Chem Soc, 132, 17004-17014, 10.1021/ja107410x, 2010.

Palmer, A. G., 3rd: Chemical exchange in biomacromolecules: past, present, and future, J Magn Reson, 241, 3-17, 10.1016/j.jmr.2014.01.008, 2014.

Rangadurai, A., Shi, H., and Al-Hashimi, H. M.: Extending the Sensitivity of CEST NMR Spectroscopy to Micro-to-Millisecond Dynamics in Nucleic Acids Using High-Power Radio-Frequency Fields, Angew Chem Int Ed Engl, 59, 11262-11266, 10.1002/anie.202000493, 2020a.

Rangadurai, A., Kremser, J., Shi, H., Kreutz, C., and Al-Hashimi, H. M.: Direct evidence for (G)O6...H2-N4(C)(+) hydrogen bonding in transient G(syn)-C(+) and G(syn)-m(5)C(+) Hoogsteen base pairs in duplex DNA from cytosine amino nitrogen off-resonance R1rho relaxation dispersion measurements, J Magn Reson, 308, 106589, 10.1016/j.jmr.2019.106589, 2019a.

Rangadurai, A., Szymaski, E. S., Kimsey, I. J., Shi, H., and Al-Hashimi, H. M.: Characterizing micro-to-millisecond chemical exchange in nucleic acids using off-resonance R1rho relaxation dispersion, Prog Nucl Magn Reson Spectrosc, 112-113, 55-102, 10.1016/j.pnmrs.2019.05.002, 2019b.

Rangadurai, A., Shi, H., Xu, Y., Liu, B., Abou Assi, H., Zhou, H., Kimsey, I., and Al-Hashimi, H.: delta-Melt: Nucleic acid conformational penalties from melting experiments, bioRxiv, 2020b.

Rangadurai, A., Zhou, H., Merriman, D. K., Meiser, N., Liu, B., Shi, H., Szymanski, E. S., and Al-

https://doi.org/10.5194/mr-2021-58
Preprint. Discussion started: 20 July 2021


Open Access MAGNETIC RESONANCE Discussions

Hashimi, H. M.: Why are Hoogsteen base pairs energetically disfavored in A-RNA compared to B-DNA?, Nucleic Acids Res, 46, 11099-11114, 10.1093/nar/gky885, 2018.

Sathyamoorthy, B., Lee, J., Kimsey, I., Ganser, L. R., and Al-Hashimi, H.: Development and application of aromatic [(13)C, (1)H] SOFAST-HMQC NMR experiment for nucleic acids, J Biomol NMR, 60, 77-83, 10.1007/s10858-014-9856-9, 2014.

Sathyamoorthy, B., Shi, H., Zhou, H., Xue, Y., Rangadurai, A., Merriman, D. K., and Al-Hashimi, H. M.: Insights into Watson-Crick/Hoogsteen breathing dynamics and damage repair from the solution structure and dynamic ensemble of DNA duplexes containing m1A, Nucleic Acids Res, 45, 5586-5601, 10.1093/nar/gkx186, 2017.

Schlagnitweit, J., Steiner, E., Karlsson, H., and Petzold, K.: Efficient Detection of Structure and Dynamics in Unlabeled RNAs: The SELOPE Approach, Chemistry, 24, 6067-6070, 10.1002/chem.201800992, 2018.

Schnieders, R., Wolter, A. C., Richter, C., Wohnert, J., Schwalbe, H., and Furtig, B.: Novel (13) C-detected NMR Experiments for the Precise Detection of RNA Structure, Angew Chem Int Ed Engl, 58, 9140-9144, 10.1002/anie.201904057, 2019.

Sekhar, A., Rosenzweig, R., Bouvignies, G., and Kay, L. E.: Hsp70 biases the folding pathways of client proteins, Proc Natl Acad Sci U S A, 113, E2794-2801, 10.1073/pnas.1601846113, 2016.

Shi, H., Clay, M. C., Rangadurai, A., Sathyamoorthy, B., Case, D. A., and Al-Hashimi, H. M.: Atomic structures of excited state A-T Hoogsteen base pairs in duplex DNA by combining NMR relaxation dispersion, mutagenesis, and chemical shift calculations, J Biomol NMR, 70, 229-244, 10.1007/s10858-018-0177-2, 2018.

Shi, H., Kimsey, I., Liu, H., Pham, U., Schumacher, M. A., and Al-Hashimi, H.: Revealing A-T and G-C Hoogsteen base pairs in stressed protein-bound duplex DNA, bioRxiv, 2021.

Shi, H., Liu, B., Nussbaumer, F., Rangadurai, A., Kreutz, C., and Al-Hashimi, H. M.: NMR Chemical Exchange Measurements Reveal That N(6)-Methyladenosine Slows RNA Annealing, J Am Chem Soc, 141, 19988-19993, 10.1021/jacs.9b10939, 2019.

Singh, U. S., Moe, J. G., Reddy, G. R., Weisenseel, J. P., Marnett, L. J., and Stone, M. P.: 1H NMR of an oligodeoxynucleotide containing a propanodeoxyguanosine adduct positioned in a (CG)3 frameshift hotspot of Salmonella typhimurium hisD3052: Hoogsteen base-pairing at pH 5.8, Chem Res Toxicol, 6, 825-836, 10.1021/tx00036a012, 1993.

Smith, C. A., Ban, D., Pratihar, S., Giller, K., Schwiegk, C., de Groot, B. L., Becker, S., Griesinger, C., and Lee, D.: Population shuffling of protein conformations, Angew Chem Int Ed Engl, 54, 207-210, 10.1002/anie.201408890, 2015.

Snoussi, K. and Leroy, J. L.: Imino proton exchange and base-pair kinetics in RNA duplexes, Biochemistry, 40, 8898-8904, 10.1021/bi010385d, 2001.

Sripakdeevong, P., Cevec, M., Chang, A. T., Erat, M. C., Ziegeler, M., Zhao, Q., Fox, G. E., Gao, X., Kennedy, S. D., Kierzek, R., Nikonowicz, E. P., Schwalbe, H., Sigel, R. K., Turner, D. H., and Das, R.: Structure determination of noncanonical RNA motifs guided by (1)H NMR chemical shifts, Nature methods, 11, 413-416, 10.1038/nmeth.2876, 2014.

https://doi.org/10.5194/mr-2021-58
Preprint. Discussion started: 20 July 2021

Open Access MAGNETIC RESONANCE Discussions

1064 Steiner, E., Schlagnitweit, J., Lundstrom, P., and Petzold, K.: Capturing Excited States in the Fast-
1065 Intermediate Exchange Limit in Biological Systems Using (HNMR)-H-1 Spectroscopy, Angew
1066 Chem Int Edit, 55, 15869-15872, 10.1002/anie.201609102, 2016.
1067 Stelling, A. L., Xu, Y., Zhou, H., Choi, S. H., Clay, M. C., Merriman, D. K., and Al-Hashimi, H. M.:
1068 Robust IR-based detection of stable and fractionally populated G-C(+) and A-T Hoogsteen base
1069 pairs in duplex DNA, FEBS Lett, 591, 1770-1784, 10.1002/1873-3468.12681, 2017.
1070 Swails, J., Zhu, T., He, X., and Case, D. A.: AFNMR: automated fragmentation quantum mechanical
1071 calculation of NMR chemical shifts for biomolecules, Journal of biomolecular NMR, 63, 125-139,
1072 10.1007/s10858-015-9970-3, 2015.
1073 Tateishi-Karimata, H., Nakano, M., and Sugimoto, N.: Comparable stability of Hoogsteen and
1074 Watson-Crick base pairs in ionic liquid choline dihydrogen phosphate, Sci Rep, 4, 3593,
1075 10.1038/srep03593, 2014.
1076 Ughetto, G., Wang, A. H., Quigley, G. J., van der Marel, G. A., van Boom, J. H., and Rich, A.: A
1077 comparison of the structure of echinomycin and triostin A complexed to a DNA fragment, Nucleic
1078 Acids Res, 13, 2305-2323, 10.1093/nar/13.7.2305, 1985.
1079 Wang, A. H., Ughetto, G., Quigley, G. J., Hakoshima, T., van der Marel, G. A., van Boom, J. H., and
1080 Rich, A.: The molecular structure of a DNA-triostin A complex, Science, 225, 1115-1121,
1081 10.1126/science.6474168, 1984.
1082 Wang, S., Song, Y., Wang, Y., Li, X., Fu, B., Liu, Y., Wang, J., Wei, L., Tian, T., and Zhou, X.: The
1083 m(6)A methylation perturbs the Hoogsteen pairing-guided incorporation of an oxidized nucleotide,
1084 Chem Sci, 8, 6380-6388, 10.1039/c7sc02340e, 2017.
1085 Wang, Y., Han, G., Jiang, X., Yuwen, T., and Xue, Y.: Chemical shift prediction of RNA imino groups:
1086 application toward characterizing RNA excited states, Nat Commun, 12, 1595, 10.1038/s41467-
1087 021-21840-x, 2021.
1088 Wang, Y. S. and Ikuta, S.: Proton on-Resonance Rotating Frame Spin-Lattice Relaxation
1089 Measurements of B and Z Double-Helical Oligodeoxyribonucleotides in Solution, Journal of the
1090 American Chemical Society, 111, 1243-1248, DOI 10.1021/ja00186a013, 1989.
1091 Weininger, U., Liu, Z., McIntyre, D. D., Vogel, H. J., and Akke, M.: Specific
1092 12CbetaD(2)12CgammaD(2)S13CepsilonHD(2) isotopomer labeling of methionine to characterize
1093 protein dynamics by 1H and 13C NMR relaxation dispersion, J Am Chem Soc, 134, 18562-18565,
1094 10.1021/ja309294u, 2012.
1095 Weininger, U., Blissing, A. T., Hennig, J., Ahlner, A., Liu, Z., Vogel, H. J., Akke, M., and Lundstrom,
1096 P.: Protein conformational exchange measured by 1H R1rho relaxation dispersion of methyl groups,
1097 J Biomol NMR, 57, 47-55, 10.1007/s10858-013-9764-4, 2013.
1098 Xu, Y., McSally, J., Andricioaei, I., and Al-Hashimi, H. M.: Modulation of Hoogsteen dynamics on
1099 DNA recognition, Nat Commun, 9, 1473, 10.1038/s41467-018-03516-1, 2018.
1100 Xu, Y., Manghrani, A., Liu, B., Shi, H., Pham, U., Liu, A., and Al-Hashimi, H. M.: Hoogsteen base
1101 pairs increase the susceptibility of double-stranded DNA to cytotoxic damage, J Biol Chem, 295,
1102 15933-15947, 10.1074/jbc.RA120.014530, 2020.

https://doi.org/10.5194/mr-2021-58
Preprint. Discussion started: 20 July 2021

Open Access MAGNETIC RESONANCE Discussions

Yamazaki, T., Muhandiram, R., and Kay, L. E.: NMR Experiments for the Measurement of Carbon Relaxation Properties in Highly Enriched, Uniformly 13C,15N-Labeled Proteins: Application to 13C.alpha. Carbons, Journal of the American Chemical Society, 116, 8266-8278, 10.1021/ja00097a037, 1994.

Yuwen, T., Sekhar, A., and Kay, L. E.: Separating Dipolar and Chemical Exchange Magnetization Transfer Processes in (1) H-CEST, Angew Chem Int Ed Engl, 56, 6122-6125, 10.1002/anie.201610759, 2017a.

Yuwen, T. R., Huang, R., and Kay, L. E.: Probing slow timescale dynamics in proteins using methyl H-1 CEST, Journal of Biomolecular Nmr, 68, 215-224, 10.1007/s10858-017-0121-x, 2017b.

Zhao, B., Hansen, A. L., and Zhang, Q.: Characterizing slow chemical exchange in nucleic acids by carbon CEST and low spin-lock field R(1rho) NMR spectroscopy, J Am Chem Soc, 136, 20-23, 10.1021/ja409835y, 2014.

Zhou, H., Sathyamoorthy, B., Stelling, A., Xu, Y., Xue, Y., Pigli, Y. Z., Case, D. A., Rice, P. A., and Al-Hashimi, H. M.: Characterizing Watson-Crick versus Hoogsteen Base Pairing in a DNA-Protein Complex Using Nuclear Magnetic Resonance and Site-Specifically (13)C- and (15)N-Labeled DNA, Biochemistry, 58, 1963-1974, 10.1021/acs.biochem.9b00027, 2019.

Zhou, H., Kimsey, I. J., Nikolova, E. N., Sathyamoorthy, B., Grazioli, G., McSally, J., Bai, T., Wunderlich, C. H., Kreutz, C., Andricioaei, I., and Al-Hashimi, H. M.: m(1)A and m(1)G disrupt A-RNA structure through the intrinsic instability of Hoogsteen base pairs, Nature structural & molecular biology, 23, 803-810, 10.1038/nsmb.3270, 2016.

Zimmer, D. P. and Crothers, D. M.: NMR of enzymatically synthesized uniformly 13C15N-labeled DNA oligonucleotides, Proc Natl Acad Sci U S A, 92, 3091-3095, 10.1073/pnas.92.8.3091, 1995.